1966

Changes in Minority Carrier Lifetime in Silicon and Gallium Arsenide Resulting from Irradiations with 22- and 40-Mev Protons

Marvin E. Beatty
College of William & Mary - Arts & Sciences

CHANGES IN MINORITY CARRIER LIFETIME IN SILICON AND GALLIUM ARSENIDE RESULTING FROM IRRADIATIONS WITH 22- AND 40-MeV PROTONS

A Thesis

Presented to

The Faculty of the Department of Physics

The College of William and Mary in Virginia

In Partial Fulfillment

Of the Requirements for the Degree of

Master of Arts

By

Marvin E. Beatty III

May 1966

CHANGES IN MINORITY CARRIER LIFETIME IN SILICON AND GALLIUM ARSENIDE RESULTING FROM IRRADIATIONS WITH 22- AND 40-MeV PROTONS

A Thesis

Presented to

The Faculty of the Department of Physics

The College of William and Mary in Virginia

In Partial Fulfillment

Of the Requirements for the Degree of

Master of Arts

By

Marvin E. Beatty III

May 1966

APPROVAL SHEET

This thesis is submitted in partial fulfillment of

the requirements for the degree of

Master of Arts

Marvin E. Beatty III

Author

Approved, May 1966:

Harlan E. Lehmann

George S. Opelt

Howard R. Gordon

ACKNOWLEDGMENT

The work reported herein was performed by the author as an employee of the National Aeronautics and Space Administration at Langley Station, Hampton, Virginia. The author is grateful to the National Aeronautics and Space Administration for endorsement of this effort.

TABLE OF CONTENTS

LIST OF TABLES

LIST OF FIGURES

Figure Page

ABSTRACT

A method is developed using an infrared light source to determine the minority carrier lifetime in the base material of a silicon and gallium arsenide P-N junction. This method is used to determine the lifetime of holes in N-type gallium arsenide, electrons in P-type silicon, and holes in N-type silicon. The effects of 22- and 40-MeV proton irradiation on the minority carrier lifetime of these materials is investigated.

The results of these investigations show that initial lifetimes in both types of silicon are on the order of 10^{-6} seconds, while for gallium arsenide it is on the order of 10^{-9} seconds initially. The radiation damage study depicts the gross differences in lifetime reduction between the three types of semiconductors. Gallium arsenide is much less sensitive to radiation damage with P-type silicon being less damaged than N-type.

The final outcome of the investigation yields a powerful tool for investigating materials having low initial minority carrier lifetimes such as gallium arsenide. The possibilities of using gallium arsenide instead of silicon for useful devices subjected to a radiation atmosphere is discussed.

CHANGES IN MINORITY CARRIER LIFETIME IN SILICON AND GALLIUM ARSENIDE RESULTING FROM IRRADIATIONS WITH 22- AND 40-MeV PROTONS

INTRODUCTION

The importance of extensive radiation damage studies with semiconductor materials is verified by the fact that these materials undergo severe changes in their useful physical properties when bombarded by ionizing radiation. Since a great many devices used in the electronic circuitry of space vehicles are composed of semiconductor materials, and depend on the physics of semiconductor action, space radiation presents a formidable problem to space exploration.

In order to construct devices less sensitive to the space radiation (trapped protons and electrons, solar flares, nuclear explosions, etc.), it is essential that the changes in the physics of semiconductor material under radiation bombardment be understood.

The sensitivity of the minority carrier lifetime to electron irradiated silicon is pointed out in references 1-6. A smaller amount of research has been carried out with protons. It is believed that, since gallium arsenide makes use of a direct transition for its current carriers, it will be damaged much less by radiation than silicon. Gallium arsenide also has a greater potential for some semiconductor devices such as solar cells, diodes, and so forth, than silicon.

The effective use of particle accelerators and cyclotrons to simulate space radiation effects has been proven by experiments in the references given. The major damage to semiconductors from protons occurs for energies up to 50-MeV (ref. 7). It just so

happens that two of the more readily available proton production machines are the 40-MeV linear accelerator at the University of Minnesota and the 22-MeV cyclotron at Oak Ridge National Laboratories, Oak Ridge, Tennessee. Both of these machines are very capable for radiation damage studies in semiconductors.

It was decided that, since the lifetime of the minority carrier was a sensitive property of radiation damage, this quantity would be measured during radiation bombardment, and used as a damage probe to determine the effects of radiation on semiconductor materials. It was also decided to determine some means of measuring the lifetime during proton irradiation as well as before and after. This has been done with electrons (ref. 8), but the method is not applicable to proton studies, therefore, no inbeam proton changes of the minority carrier lifetime in semiconductors have been made.

Also, there has been very little radiation damage work done in gallium arsenide, and virtually no studies made using proton bombardment in determining change in the minority carrier lifetime.

Keeping these facts in mind the following experiments were planned:

N- and P-type silicon.- It would be advantageous to look at these two widely used semiconductors using the new method for determining changes in the lifetime. As was mentioned before, no lifetime measurements in semiconductors have been reported during irradiation by protons to the authors knowledge. There has also been little work in silicon using 22- and 40-MeV protons for other measurements.

Results from the silicon tests could be compared to the results in gallium arsenide to determine if GaAs is less damaged by radiation than silicon (at least for the energies tested).

It is hoped that data obtained from this study of silicon will add to and support existing data.

P-type gallium arsenide.- At the present stage of development, P-type gallium arsenide is easier to fabricate and more widely used than N-type.

Since N-type is difficult to obtain and results would depend heavily on impurity variation from sample to sample, it was decided to work exclusively with P-type GaAs for this experimental study. As fabrication of N-type GaAs improves, future studies will investigate this material.

CHAPTER I

THEORY

Nucleon Irradiation of Solid Materials

Solid materials are affected by practically all types of radiation. The basic chemical structures of many of these materials are seriously altered by bombardment with energetic particles (neutrons, protons, deuterons, alpha particles, etc.). Defects which are produced by these radiation particles in the structure of a solid material will affect the macroscopic properties of the solid in varying degrees. It follows, then, that a study of defects introduced in the lattice of a solid by irradiating particles (radiation damage) can be useful in furthering the existing knowledge of the structure of solids. Understanding the effects of radiation damage in solids requires techniques and theories from other areas of experimental studies such as nuclear physics involving production and decay of transmuted atoms in the solid, and a knowledge of the electronic structure of the atoms involved in the excitation or ionization process as the particles pass through the solid. The various processes which are important in producing changes in the lattice structure of solids must be understood. The following major processes will be considered for proton penetration of a semiconductor lattice:

Ionization effects.- A proton passing through matter loses most of its energy by ionization and excitation of electrons in the atoms of the material. This process can cause the creation of electron-hole pairs in semiconductors. This effect is actually of a transient nature, since the excess energy is quickly dissipated throughout the material and the electron-hole pairs recombine to form a neutral site. Transient effects can be important when the resistance produced can form a barrier to normal conduction of minority and majority carriers in semiconductors.

Transmutations.- It is possible for protons with sufficient energy which are passing through a semiconductor to cause direct nuclear transmutations which could act as substitutional impurities in the lattice. An example of this would be the irradiation of germanium by Lark-Horovitz (ref. 9) in which the thermal neutrons produced a P-type semiconductor by the introduction of gallium in excess of arsenic as the end product of nuclear transmutation. But, since this experiment, it has been found that the transmutation products are not important in the proton damage process.

When considering the energies of protons which might be the most damaging to semiconductors, the total cross section (elastic and inelastic scattering) of proton collision with semiconductor atoms must be accounted for. Using the cross-section for silicon at about 50-MeV proton energy as an upper limit, the number of transmutations produced can be calculated:

$$\sigma = \pi r^2 \qquad (1)$$

where σ is the true cross section at any energy, and r is the nuclear radius.

$$r = A^{1/3} \left(1.4 \times 10^{-13} \text{ cm}\right) \cong 4 \times 10^{-13} \text{ cm} \qquad (2)$$

Therefore,

$$\sigma = 5 \times 10^{-25} \text{ cm}^2.$$

If it is considered that all interactions will produce recombination centers (worst case), then the number of transmutations produced is

$$N_T = N_{Si}\, \sigma = 0.025 \text{ cm}^{-1} . \qquad (3)$$

This is a small number of defects compared to lattice displacement which ranges from 2.0 cm^{-1} for 180-MeV protons to 40.0 cm^{-1} for 4-MeV proton irradiation.

Since all semiconductor materials have simular structure $\left(\sigma_{Ga} \simeq \sigma_{As} \simeq 4.5 \times 10^{-25} \text{ cm}^2 \text{ and } N_T \approx 0.03\right)$, transmutation production may be neglected when considering proton damage in the energy range 0 - 180-MeV.

Lattice displacement.-

1. General theory. Low energy protons and electrons can produce the simplest type of defects in a semiconductor, that is, vacancy-interstitial pairs (Frenkel defects). This involves an elastic scatter of charged particles by a nucleus. If a lattice atom can receive enough energy by its nucleus, it can break the bonds which

normally hold it in position, and move to some interstitial site within the lattice. The diamond-type lattice of semiconductors is open, and the energy needed to displace an atom is only approximately 15.0 eV.

2. Heavy particle effects. Again consider the silicon lattice as characteristic of all semiconductor material. Consider also a monoenergetic proton beam striking a sample sufficiently small in size that the energy loss to the beam is small. At low energy, theory predicts a simple Rutherford scattering process in which the cross-section decreases rapidly as 1/E. But, there is a certain energy above which the non-Rutherford scattering process will dominate. This energy is estimated at around 100-MeV, but it is believed the energy is much lower than this.

The classical differential cross-section for Rutherford scattering is

$$\frac{d\sigma}{d\Omega} = \frac{\pi b^2}{16} \frac{1}{\sin^4 \frac{\theta}{2}} \tag{4}$$

where b is the classical distance of closest approach. θ is the proton deflection angle, Ω is the solid angle of approach.

$$b = \frac{2Z_1 Z_2 \epsilon^2}{\mu v^2} \tag{5}$$

where $Z_1\epsilon$ and $Z_2\epsilon$ are electrical charges of the incident particle and the target nucleus.

μ is the reduced mass

v is the velocity of the incident particle (lab. system).

Local disorder and defects.-

1. General theory. At present, the knowledge concerning radiation defect production in the silicon lattice is better understood than any other semiconductor. Investigations made with silicon have pointed out two major types of defect complexes, the oxygen-vacancy and the donor-vacancy-interstitial pairs created by protons and other radiation particles which can diffuse away from the point where they were produced. They can combine with each other and other types of crystal impurities (spikes, dislocations, foreign atoms, etc.) to form electrically active centers. The nature of these centers and which type is most detrimental to electrical conductivity in semiconductors is poorly understood. The studies referenced above have given complexes such as the A-center (an interstitial oxygen atom plus a vacancy), the E-center (a phosphorous donor atom plus a vacancy), and the C- and J-centers (different states of the divacancy). These are only a few of the many centers produced by radiation, and so far there is no way of predicting which of these types will dominate a particular semiconductor material during irradiation (see ref. 10-13).

Heavy particles (e.g. protons) give a greater average energy to the primary recoils which must be lost in subsequent production of displacements. The displacement cascade occurs over distances comparable to the range of the primary recoil; severely disordered regions (high defect density whose linear dimensions are 100 - 200Å are produced by primary recoils with energy as low as 10^4 eV. When this local defect density is high, the opportunity for mutual

interaction between defects becomes great, and a variety of complex centers can form (ref. 14).

2. Differences in N- and P-type silicon. There is some discrepancy in the threshold energy for defect production in N- and P-type silicon. In N-type silicon pulled in a quartz crucible, it was found that the impurity oxygen was in large abundance ($\sim 10^{18}$ cm^{-3}). This can result in a large production of A-centers (oxygen-vacancy complex) upon irradiation, and gives an acceptor level at Ec-0.17 eV (where Ec is the energy of the bottom of the conduction band). In N-type silicon grown in vacuum by float zone (FZ), there is an abundance of a donor impurity such as phosphorous present. This can cause the creation of E-centers (donor-vacancy complex), and gives an acceptor level at Ec-0.40 eV upon irradiation.

It would be expected that P-type silicon would behave in a similar manner with the exception that the impurity levels in P-type silicon are donors and are located above the valence band. This was found to be true, but radiation damage studies measuring changes in conductivity gave a profound difference in the amount of damage resulting from equivalent radiations of N- and P-type silicon. The only solution available to this discrepancy was that the rates of introduction of complex centers by radiation was different for the two types.

There are other forms of damage besides vacancy-interstitial production, but of lesser importance. One of these is extreme heat generated in a small area as a particle passes through. The heat

causes the area to expand as the particle passes through. After the particle passes, the area cools very rapidly or "quenches". This can result in a disorder in the lattice and is often referred to as a "thermal spike."

The main forms of damage in semiconductors have been presented in order that a proper interpretation of radiation damage in the experiments to be performed may be made.

Fundamentals of Semiconductors

Band structure of semiconductors.- The thermal, optical, and electrical properties of semiconductors can best be explained by using band theory. This theory states that the energy levels in a crystal which has no defect centers must stay in certain "bands" of allowed energies which are separated by forbidden energy bands where the electron may not exist.

In dealing with semiconductors, there is need to consider only three main energy bands. They are the uppermost filled band called the valence band, the forbidden band (gap) just above the valence band and completely empty, and a band just above the forbidden gap called the conduction band. This band is normally empty, but as the temperature is raised in the lattice, more and more electrons receive sufficient energy to surmount the forbidden gap, and enter the conduction band. As the name implies, the electrons in the conduction band are free to wander through the crystal and conduct a current. Likewise, in the valence band, the electrons which were thermally excited across the forbidden gap left a quantity known as a "hole". A simple definition of the hole is the absence of

an electron in a position that desires to possess an electron. As a result when a field is applied to a semiconductor in some manner, electrons in the valence band can move by jumping into the holes, and in turn leave a hole where it was originally located. In solid state physics this flow of current in the valence band is termed "hole flow" since the electrons move freely only if the holes are present. The hole has exactly the same charge as the electron, but of positive sign. Hole current is observed as a flow opposite in direction to the normal electron flow.

Considering the case where the concentration of electrons in the conduction band is small, a statistical treatment of the bands will yield the concentration of electrons and holes, thus,

$$N_e = \frac{2}{h^3} \left(2\pi\, m_e\, KT\right)^{3/2} \exp - \frac{\left(E_g - E_F\right)}{KT} \tag{5}$$

and,

$$N_h = \frac{2}{h^3} \left(2\pi\, m_h\, KT\right)^{3/2} \exp - \frac{E_F}{KT} \tag{6}$$

where,

T = absolute temperature

E_F = Fermi level

N_e = electron concentration in the conduction band

N_h = hole concentration in the valence band

m_e = electron effective mass

m_h = hole effective mass.

By introducing impurities into the crystal, the lattice can be made to have localized defect energy levels within the forbidden gap

(see fig. 1). Figure 1(a) displays the normal band picture of a pure or intrinsic crystal lattice. Figure 1(b) shows a donor level within the forbidden gap, which can give electrons to the conduction band when thermally excited. Figure 1(c) shows an acceptor level within the forbidden gap which provides holes in the valence band by attracting electrons from it. Both of the processes shown in figure 1(b) and 1(c) can increase the conduction in a semiconductor. A semiconductor of the type in figure 1(b) is called N-type with excess electrons. Figure 1(c) is an example of a P-type semiconductor with excess holes.

The probability that any localized level E is occupied by a carrier is given by the Fermi-Dirac distribution function:

$$f(E) = \frac{1}{1 + \exp\left(\frac{E - E_F}{KT}\right)} \tag{7}$$

where,

f(E) = probability that a state E is occupied

E_F = Fermi level (or energy)

K = Boltzmann's constant

T = absolute temperature.

Minority carrier lifetime.-

1. Basic theory. The lifetime of minority carriers in a semiconductor material is defined as the average time that excess minority carriers (holes or electrons) will exist before they are reduced to a factor of 1/e of their original number due to the recombination process.

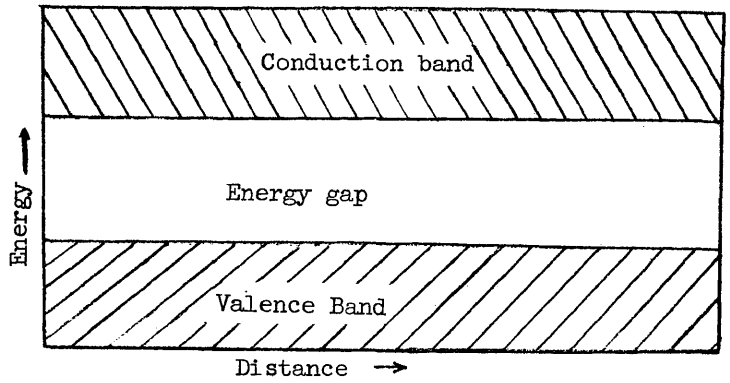

(a) Intrinsic.

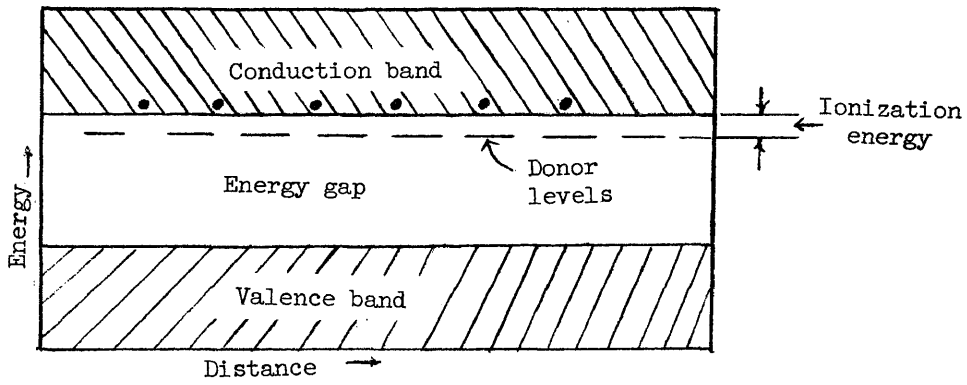

(b) Donor level.

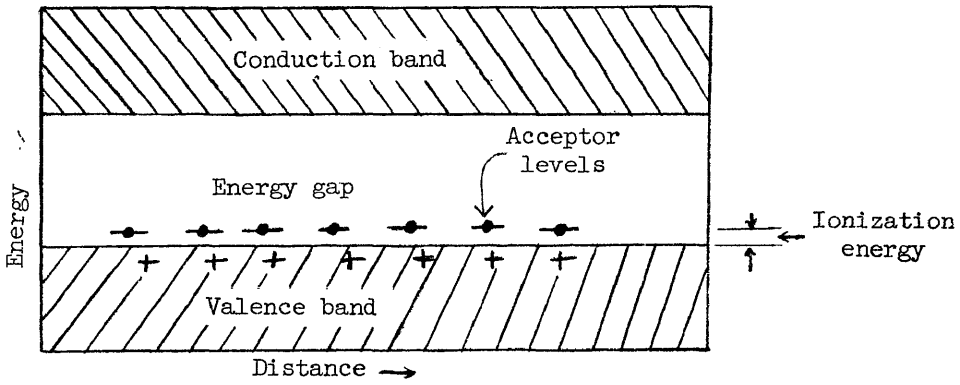

(c) Acceptor level.

Figure 1.- Energy levels in semiconductors, (a) intrinsic, (b) N-type, (c) P-type.

The Shockley-Read theory (ref. 15) gives the basic formulas for the recombination of excess carriers. According to this theory, energy levels localized deep in the forbidden gap will govern the recombination process. The lifetime, τ, when more than one energy level is present is given by

$$\tau^{-1} = \sum_i \tau_i^{-1} \tag{8}$$

in which, the τ_i are lifetimes due to each level.

Minority carrier capture is usually a rate limiting part of the recombination process for particular centers. An example of this is the rate of decrease of holes in N-type material,

$$-\frac{d}{dt}\Delta p = \sigma_p v_p N_R f_R \Delta_p \tag{9}$$

where,

Δ_p = the concentration of holes in excess of the equilibrium concentration

σ_p = the cross-section for hole capture by the particular center in question

v_p = thermal velocity of holes

N_R = total concentration of the type of recombination center being considered

f_R = the fraction of centers occupied by electrons (the fraction that may attract holes and capture them).

From Shockley-Read theory,

$$\tau_p = \frac{\Delta_p}{\frac{d}{dt}\Delta p} = \frac{1}{\sigma_p v_p N_R f_R} \tag{10}$$

The above expressions apply to recombination only when the defect level lies in the upper half of the band gap. If this is not the case, then the hole could escape to the valence band before the electron arrived to annihilate it.

The same type of equations would apply to electrons for levels in the bottom half of the forbidden band of P-type material. Then all the terms would be for electrons instead of holes. According to Shockley-Read theory, both hole and electron recombination equations may be combined into one recombination equation,

$$\tau = \frac{\tau_{Po}\left(N_1 + N_o\right) + \tau_{No}\left(P_1 + P_o\right)}{N_o + P_o} \qquad (11)$$

where,

N_o, P_o = equilibrium concentration of electrons and holes, respectively

N_1, P_1 = number of electrons and holes, respectively, above the equilibrium concentration

and,

$$\tau_{P_o}^{-1} = \sigma_p v_p N_R \qquad \text{(for holes)}$$

and,

$$\tau_{No}^{-1} = \sigma_n v_n N_R \qquad \text{(for electrons).}$$

2. Radiation effects. Radiation-induced defect centers provide recombination and trapping centers for minority carriers. Since the lifetime depends on time required for recombination of the excess minority carriers which are generated by some form of excitation (γ-rays, low energy photons, electrons, etc.), it can readily be seen that, any disturbance which affects recombination rate will produce a corresponding change in the lifetime. For this reason, τ is more

sensitive to radiation damage than most other electrical measurements in semiconductors. It is possible that as few as 10^{10} defects/cm^3 may be detected using determination of τ (ref. 16). Hall (ref. 17) and Shockley and Read (ref. 15), have demonstrated the sensitivity of τ to the introduction of energy levels near the center of the forbidden gap by proton irradiation in silicon. They have found that concentrations of energy levels on the order of 10^{12} cm^{-3} are detected using changes in τ.

The introduction of recombination centers by irradiation reduces the lifetime. If the irradiation flux is kept at low levels, then the assumption can be made that the number of recombination centers introduced will be proportional to the flux bombardment time and capture cross-section for the minority carriers at the particular energy of the particles. The reduction of the lifetime can yield a direct indication of the number of recombination centers being introduced by radiation bombardment.

P-N junction theory and the photovoltaic effect.- A P-N junction consists of a single semiconductor crystal which has adjacent areas of P- and N-type semiconductor. When this occurs, the majority carriers (electrons in N-type and holes in P-type) flow across the junction because of their mutual attraction. This flow leaves the N-type region with net positive charge, and the P-type region with net negative charge. This sets up a field which opposes the continued flow of majority carriers. When the system is in equilibrium, the field will just balance the effect of the concentration gradient set up by majority-carrier flow (see fig. 2(a)). The net charges are seen immediately adjacent to the junction in an

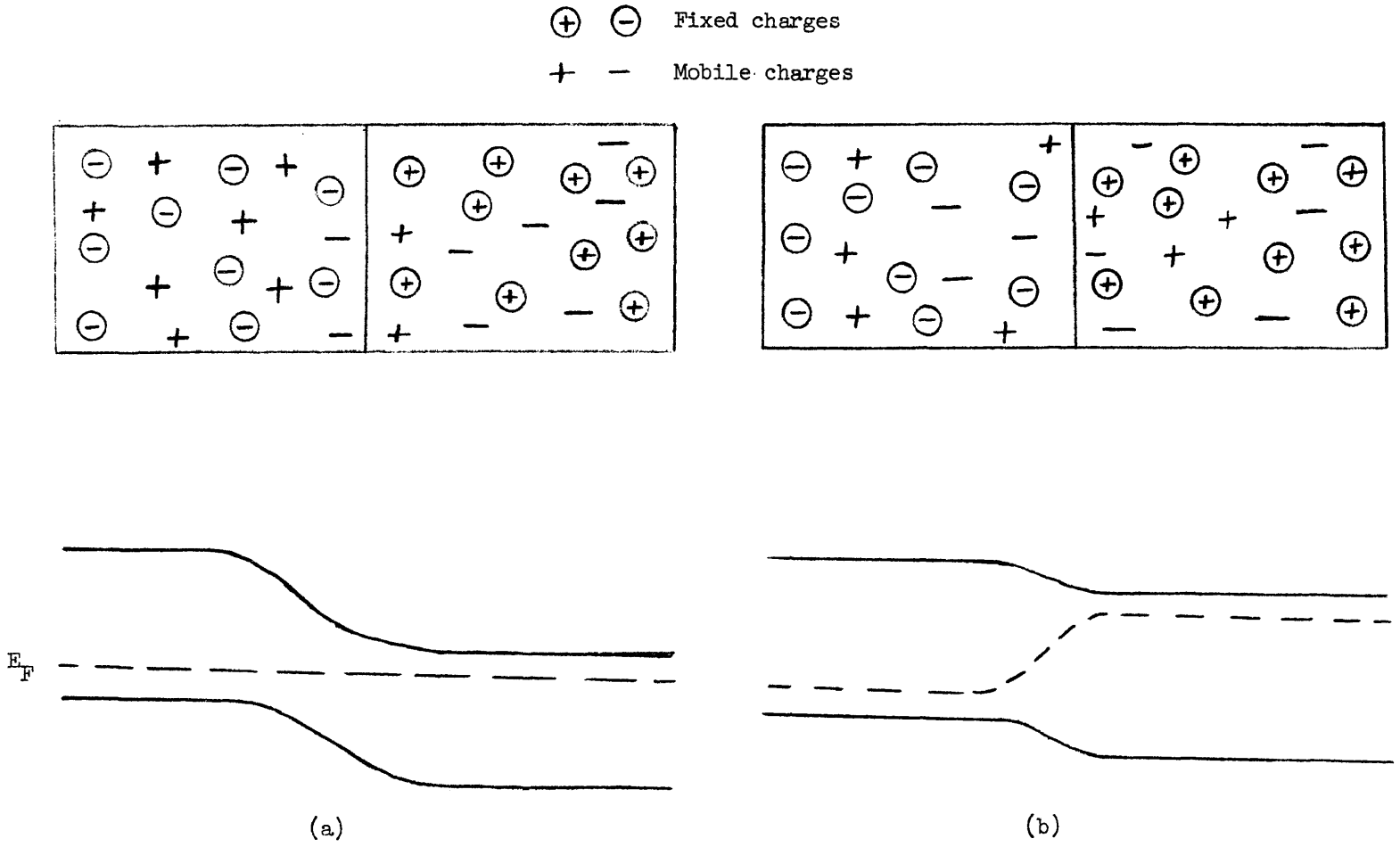

Figure 2.- P-N junction; (a) equilibrium condition, (b) excitation by photons, and so forth (forward bias). P-region is on the left, N-region on the right.

area called the space-charge region. The field also appears in this area.

The Fermi levels in the N and P regions must be equal at equilibrium. This sets up the potential difference between the two regions. At equilibrium there are a few electrons that receive enough thermal energy to leave the N-type and cross the junction into the P-type. But, at the same time, there are fixed electrons in the P-type generated thermally that are attracted to the N-type region by the net positive charge at the junction on the N-type side. The result of these two processes is no net electron or hole current. Figure 2(b) shows the effect of an applied positive potential. The potential barrier between the two regions is lowered as can be seen by the change in the Fermi level. This means that the forward currents of both holes and electrons are greatly increased, and there is a net current flow across the junction.

Figure 2 is a type of material in which the concentration of electrons on the N side and holes on the P side are about equal. However, one side could be more heavily doped than the other. This would cause a high injection of carriers of larger concentrations toward the side with smaller concentration of opposite type carriers. This would create a large current to be collected.

The current across the junction can be approximated by

$$I = I_s \left[\exp (qV/KT) - 1\right] \qquad (12)$$

where

I_s = the saturation current.

Gallium arsenide characteristics.- Gallium arsenide is a semiconductor compound of the III - V variety. Its characteristics are quite different from those of silicon. The crystals which are available for study at present are not as pure as those of silicon.

The major difference between gallium arsenide and silicon lies in the difference in their band structure. There are two major differences between gallium arsenide and silicon bands. First, the minimum width of the forbidden energy is larger for gallium arsenide than for silicon (1.32 eV for GaAs, and 1.04 eV for Si). Second, the energy maximum in the valence band lies in the same direction in wave vector or "K" space as the minimum in the conduction band (at $\overline{K} = 0$), where K is the wave vector in the reduced brillouin zone (see fig. 3, ref. 18). This means that "direct" transitions of electrons from the valence band to the conduction band can be made. This is not the case in silicon which requires the assistance of impurity levels located within the energy gap as "stepping stones" for generation of electrons from the valence band to the conduction band.

This band structure peculiarity of GaAs makes it adaptable to many unique devices made from the material such as the diode injection laser. Also, due to the large band gap and other factors, GaAs devices will operate at higher temperatures (up to 300° C) than silicon devices of the same type (below 200° C). In photosensitive devices it is also possible to achieve a higher photovoltage (0.9 V) with GaAs than with Si (0.6 V), reference 19.

Table I gives a list of important properties of GaAs as compared to Si.

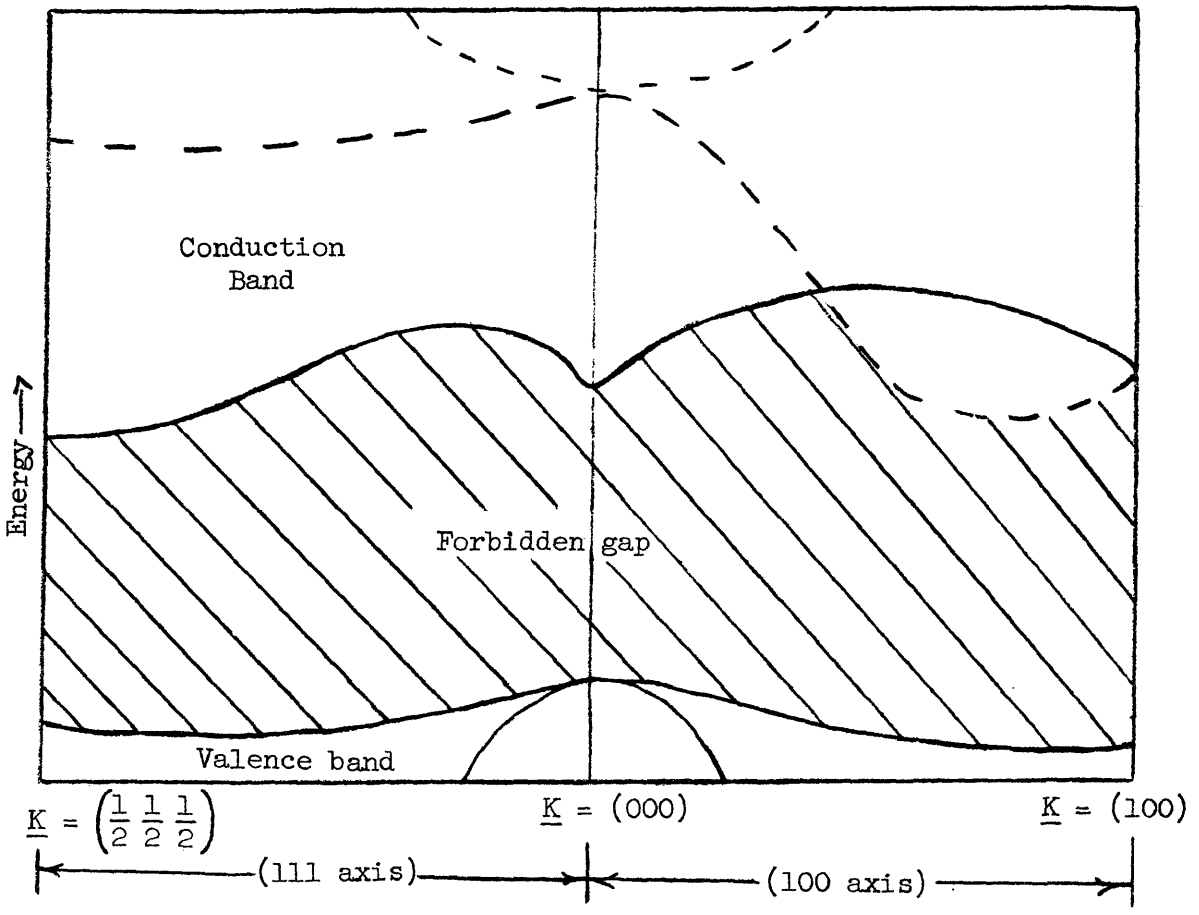

Figure 3.- Hypothetical energy band contours for gallium arsenide.

CHAPTER II

CALCULATIONS AND METHOD OF ANALYSIS

Carrier Generation by Photons in a P-N Junction

When light is absorbed by a semiconductor material, those photons with the proper energy can release an electron from an atom and create on electron-hole pair. This increases conductivity within the material. If a semiconductor is doped so as to form a P-N junction, the light can create electron-hole pairs which can diffuse to the junction and be collected as a current. This current could be used to perform some useful function.

From figure 4 the general process involved in a P-N junction can be seen when the junction is being bombarded by light. In terms of contribution of the light to increased conductivity, the following considerations are known to be true from figure 4:

1. A fraction of the incident photons are reflected.

2. Photons with very short wavelengths generate many electron-hole pairs very close to the surface. However, these pairs quickly recombine because of surface recombination (little is known about this effect except that it is very complicated and makes it almost impossible to determine the true lifetime in the surface material).

3a. Photons with wavelengths in the visible region of the spectrum generate electron-hole pairs which can diffuse to the space-charge region and contribute to the total short-circuit

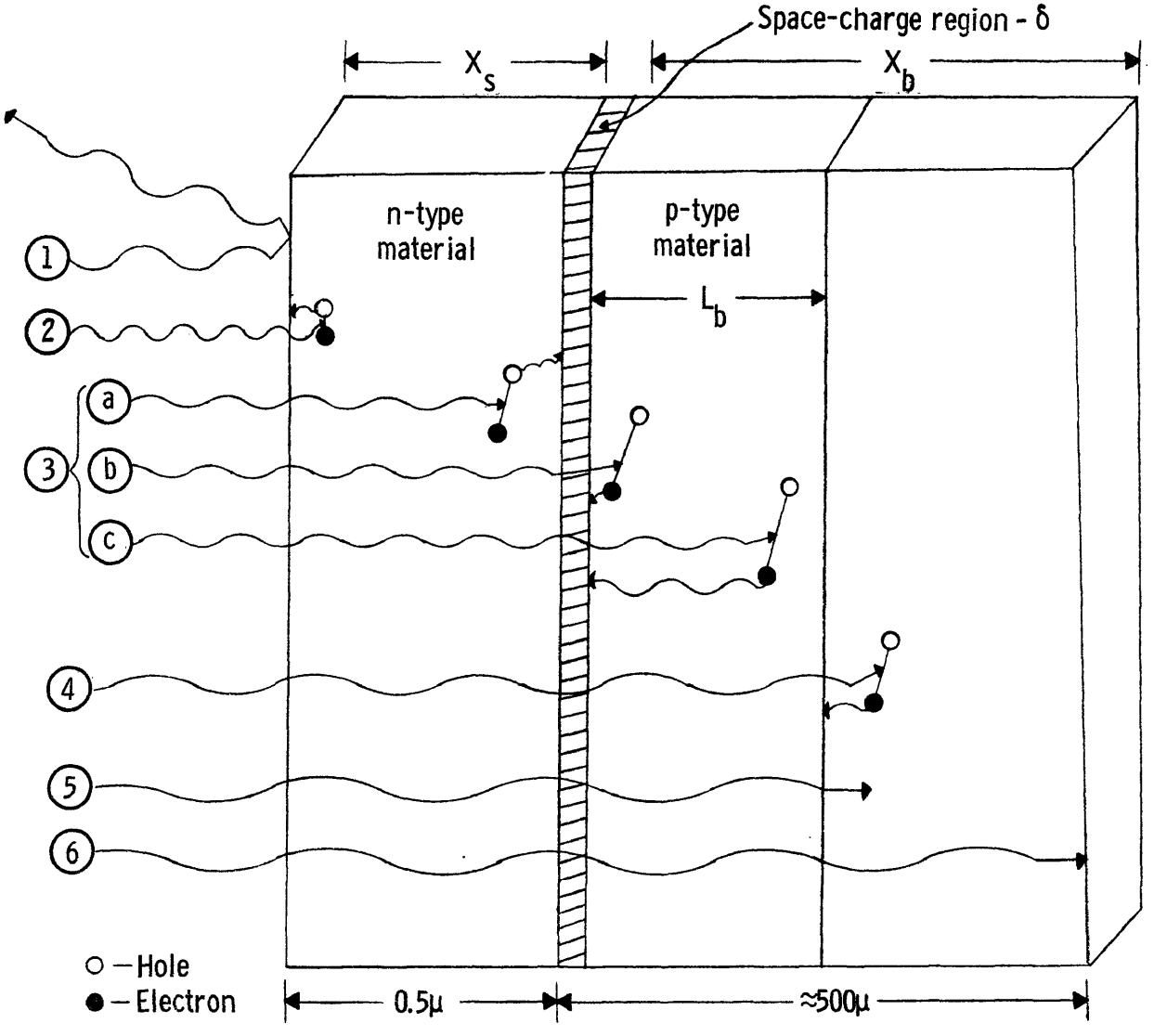

Figure 4.- P-N junction dependence on photon wavelength for current production.

current. But, since a large portion of these pairs are still being formed in the thin surface layer (~0.5μ thick), there is still a large percentage of pairs being recombined because of the high surface recombination velocity.

3b. Photons with wavelengths in the near infrared generate electron-hole pairs primarily in the base region of the cell which are within a diffusion length of the space-charge region (the diffusion length is defined as the distance moved by the minority carriers before being reduced to a factor of 1/e of their original number due to the recombination process).

3c. Photons in this part of the spectrum are used to determine measurements of diffusion length and lifetime.

4. Some pairs are formed outside a diffusion length and do not contribute to the current.

5. Photons are absorbed, but the absorbed energy is insufficient to generate electron-hole pairs.

6. The far-infrared wavelengths simply pass through the material.

From figure 4 it can be seen that a P-N junction has possibilities of being used as a tool for determining basic physical properties of semiconductors.

There is a definite relationship between the diffusion length and the lifetime of minority carrier. In the case of a uniform excitation such as by a monochromatic beam of infrared light, carriers are produced in a semiconductor in a particular region of the crystal. The steady state density of the carriers produced is measured as a function of distance from the injection point. The lifetime would be determined from the steady state solution of the diffusion equation:

$$\frac{\partial P}{\partial t} = -\frac{P}{\tau} + D_p \nabla^2 P + g' \qquad (13)$$

where,

g' = rate of generation/cm^3 by photons.

After time has elapsed, excess carriers build up due to g'. The recombination process will balance this increase in carriers, and a steady-state condition will exist,

$$\frac{\partial P}{\partial t} = g' \ . \qquad (14)$$

The differential equation becomes manageable, being second order in P,

$$P = \tau D_p \frac{\partial^2 P}{\partial X^2} \ . \qquad (15)$$

The form for linear geometry which determines the number of carriers at a length X is,

$$P = Po\ e^{-X/L_p} \ . \qquad (16)$$

Putting (16) into (15) we get,

$$Po\ e^{-X/L_p} = \frac{\tau D_p}{L_p^2} Po\ e^{-X/L_p} \qquad (17)$$

and,

$$L_p^2 = \tau D_p \ . \qquad (18)$$

Thus, it can be seen that the diffusion length and lifetime are directly related through a constant D known as the diffusion constant. If the diffusion length is known, the lifetime can be found by,

$$\tau = \frac{L^2}{D} \cdot \tag{19}$$

Calculation of the Diffusion Length

The basic diffusion equations and the current density calculated from them as a function of diffusion and recombination are presented in references 20 and 21. From these equations is developed a relation for determining the diffusion length existing in the base region of a p-n junction. This relation has the following form,

$$\frac{1}{L_b} = \alpha\left[\frac{A\ H\ (1-R)}{(h\nu)\ I} - 1\right] \tag{20}$$

where,

L_b = base material diffusion length (μ)

α = absorption coefficient (cm^{-1})

A = area of p-n junction (cm^2)

H = absolute light energy density ($watts/cm^2$)

$h\nu$ = energy of photons bombarding the junction (ev)

I = current generated in base material by incident photons (μ amps)

R = reflectance of p-n junction surface (dimensionless)

From this equation it can be seen that there is the possibility of setting up an experiment which would allow determination of the diffusion length and, therefore, the minority carrier lifetime. It shall also be possible to monitor these conduction parameters against radiation bombardment.

CHAPTER III

DISCUSSION OF EXPERIMENTAL TECHNIQUES

Selection and Preparation of Samples

Silicon.- The silicon samples used were commercially available 1.0 Ω - cm P on N and N on P solar cells. Thus, lifetime measurements for both N- and P-type silicon could be obtained. The fabrication of these samples is a standard process developed by industry and generally adhered to.

Gallium arsenide.- The gallium arsenide P-N junctions were fabricated in the form of experimental solar cells with only P on N type being available under present techniques. Therefore, the samples tested were N-type GaAs with a carrier concentration of approximately 7.3×10^{17} e^-/cm^3, a resistivity of 0.0032 Ω - cm, and a mobility of 2680 cm^2/volt-sec. The techniques used to fabricate these samples may be found in references 22 and 23. GaAs is a single crystal cut in the 1:1:1 plane and doped with germanium. The junction is formed 0.5 microns below the surface by diffusing in a mixture of 40 percent Zn: 60 percent In at 720° C for ten minutes. The leads are Ti-Ag which yielded a series resistance less than 0.5 Ω. The physical dimensions of the sample are given in figure 5.

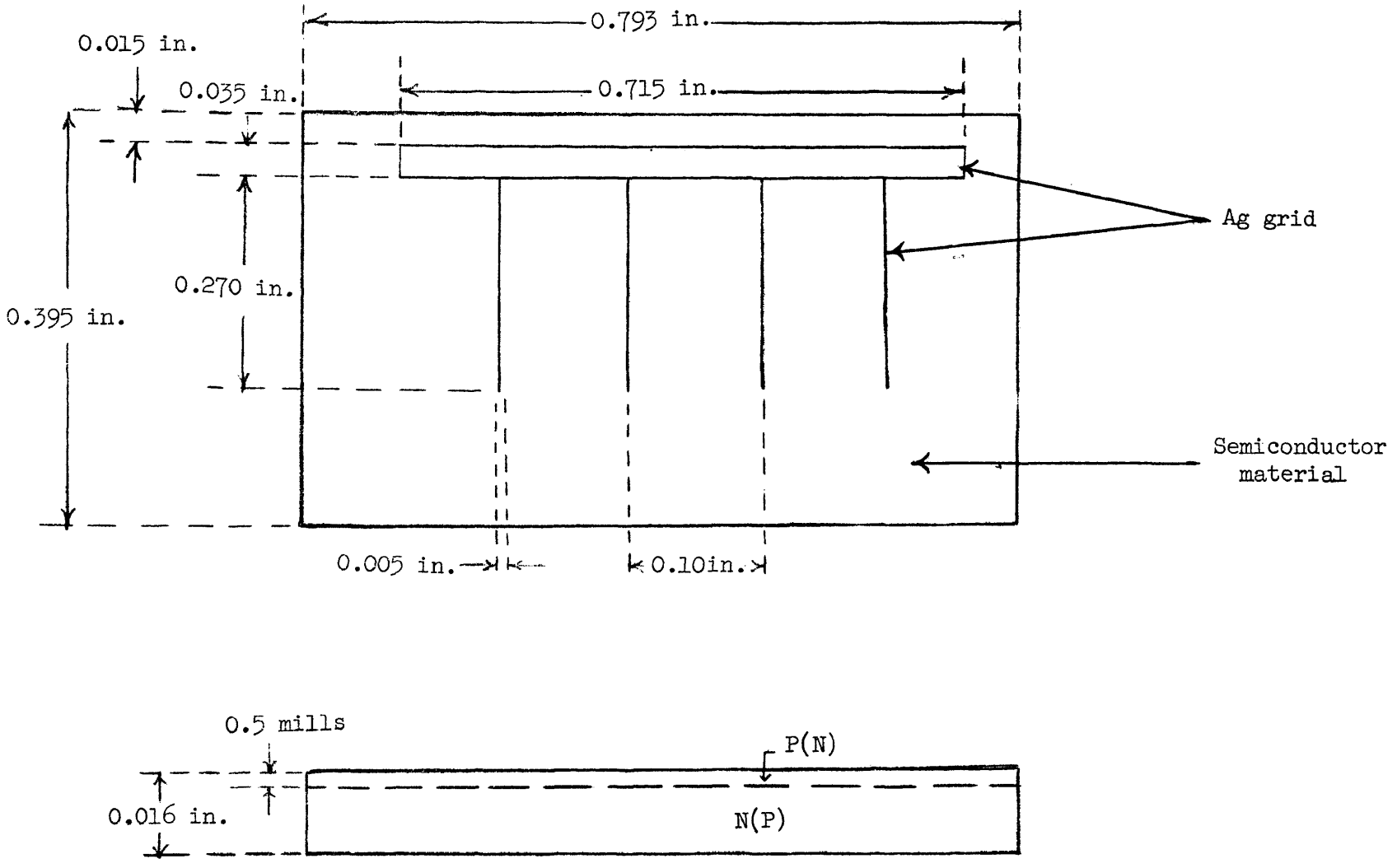

Figure 5.- Physical dimensions of samples tested. (Depth of junction and location of current collecting grids on semiconductor material)

Bombardment Chambers

The bombardment chamber used at the University of Minnesota is shown in figure 6. The plate has provisions for holding twelve samples with electrical connections available for inbeam readout. By use of a system of motors and gears, the carriage could be moved both horizontally and vertically by remote control. This allowed the samples to be placed in the beam without cutting the accelerator off, thereby increasing stability of the proton beam. The sample carriage did not have provisions for vacuum measurements.

For the Oak Ridge experiment, it was decided that a much more sophisticated chamber which would allow vacuum measurements would be designed. The experimenter, in collaboration with Mr. Harry Cupp of the Oak Ridge National Laboratory, designed the chamber shown in figure 7. This chamber also holds twelve samples. The samples are mounted on connectors and extend to the center of the beam window. The entire assembly can be operated under vacuum or in air. The targets are insulated and connected through a rotary commutator to remote electronic gear for inbeam tests. The wheel has a geneva mechanism which tells the experimenter which sample is in the beam. There are provisions for heat sinks in case temperature problems arise during irradiation. There is also a Faraday cup located in the rear of the wheel at beam position, but this was not used for beam monitoring in these tests. Figure 8 shows the chamber connected to the proton beam pipe.

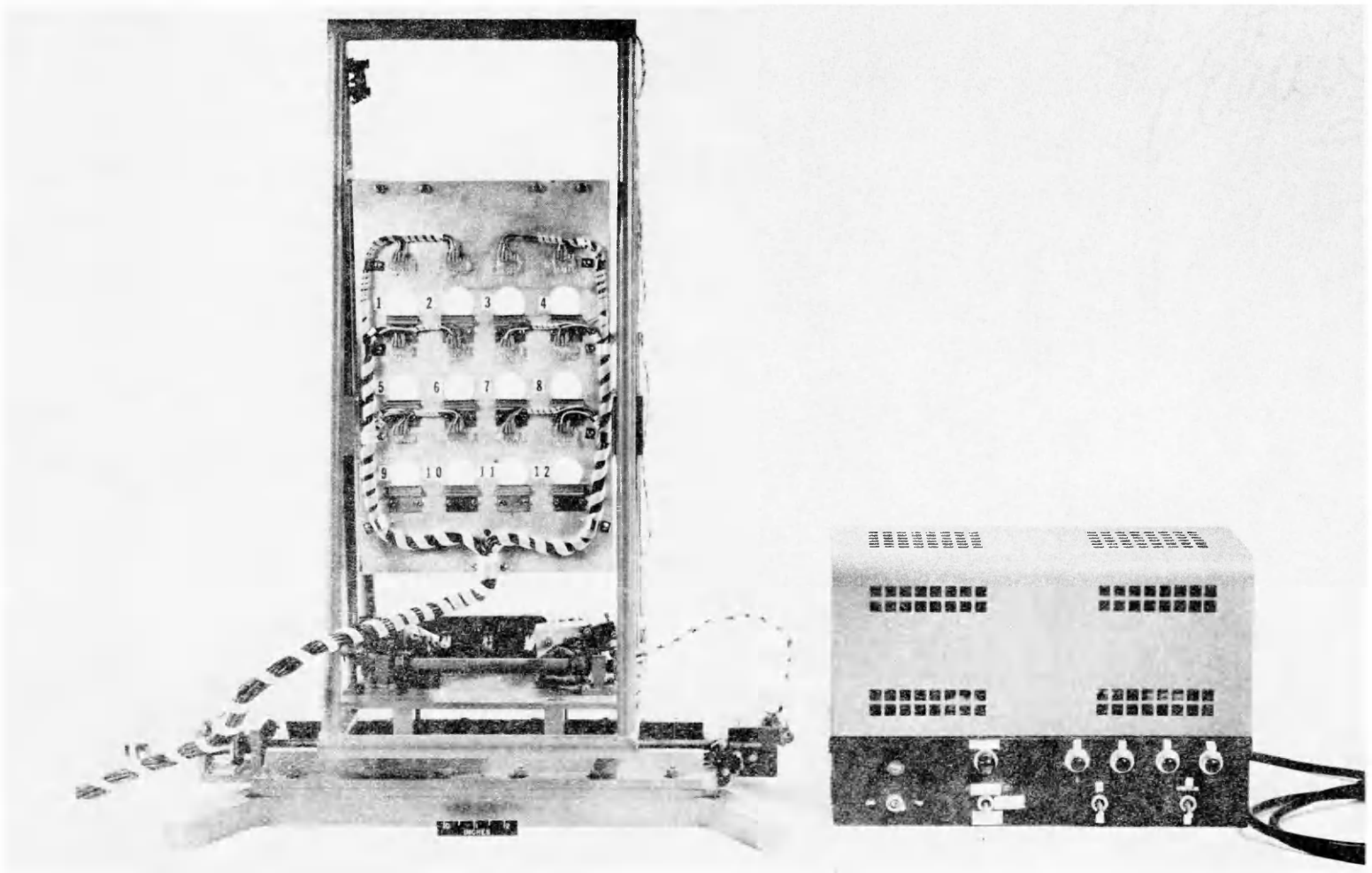

Figure 6.- Sample carriage used at the University of Minnesota.

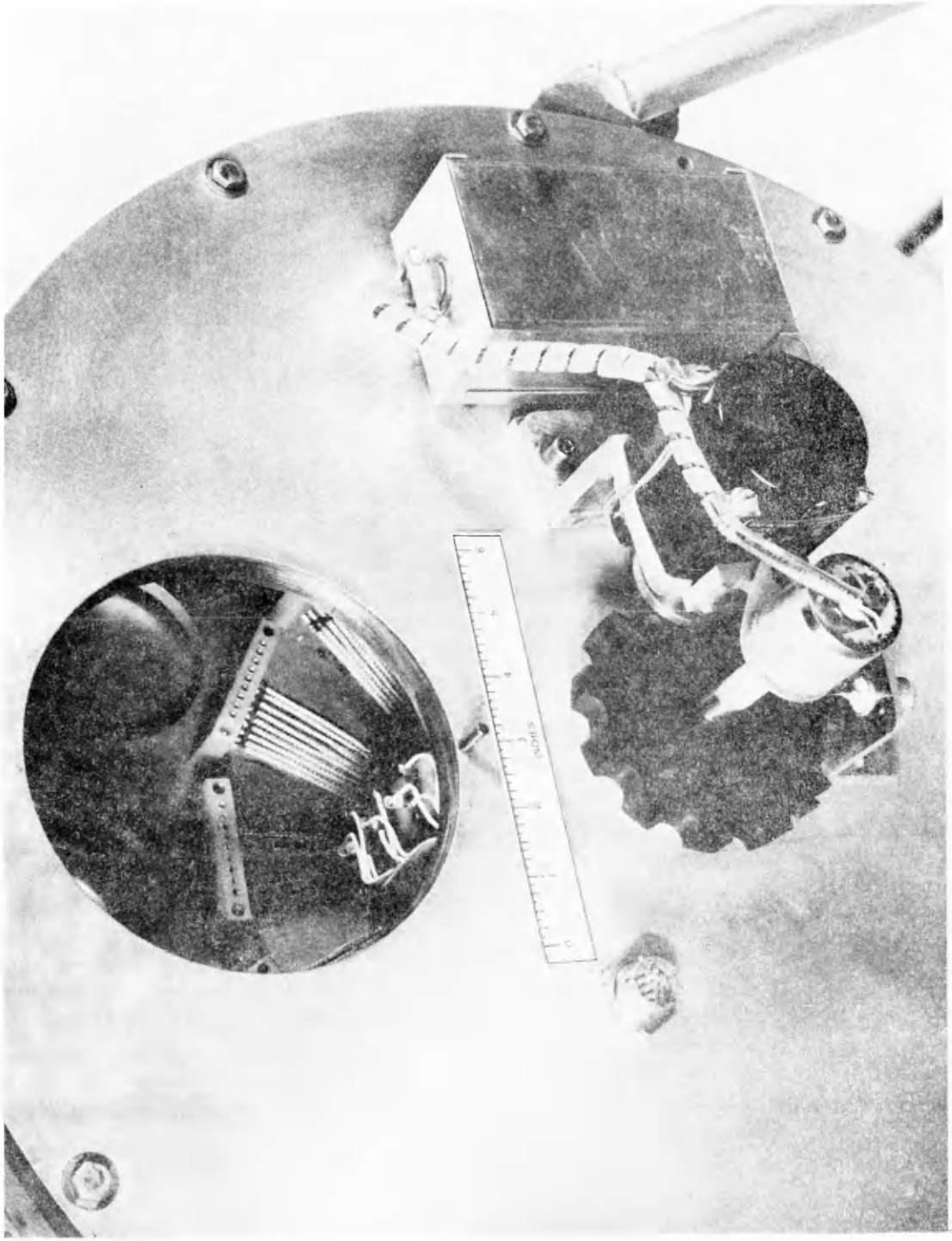

Figure 7.- Bombardment chamber used for 22-MeV proton test.

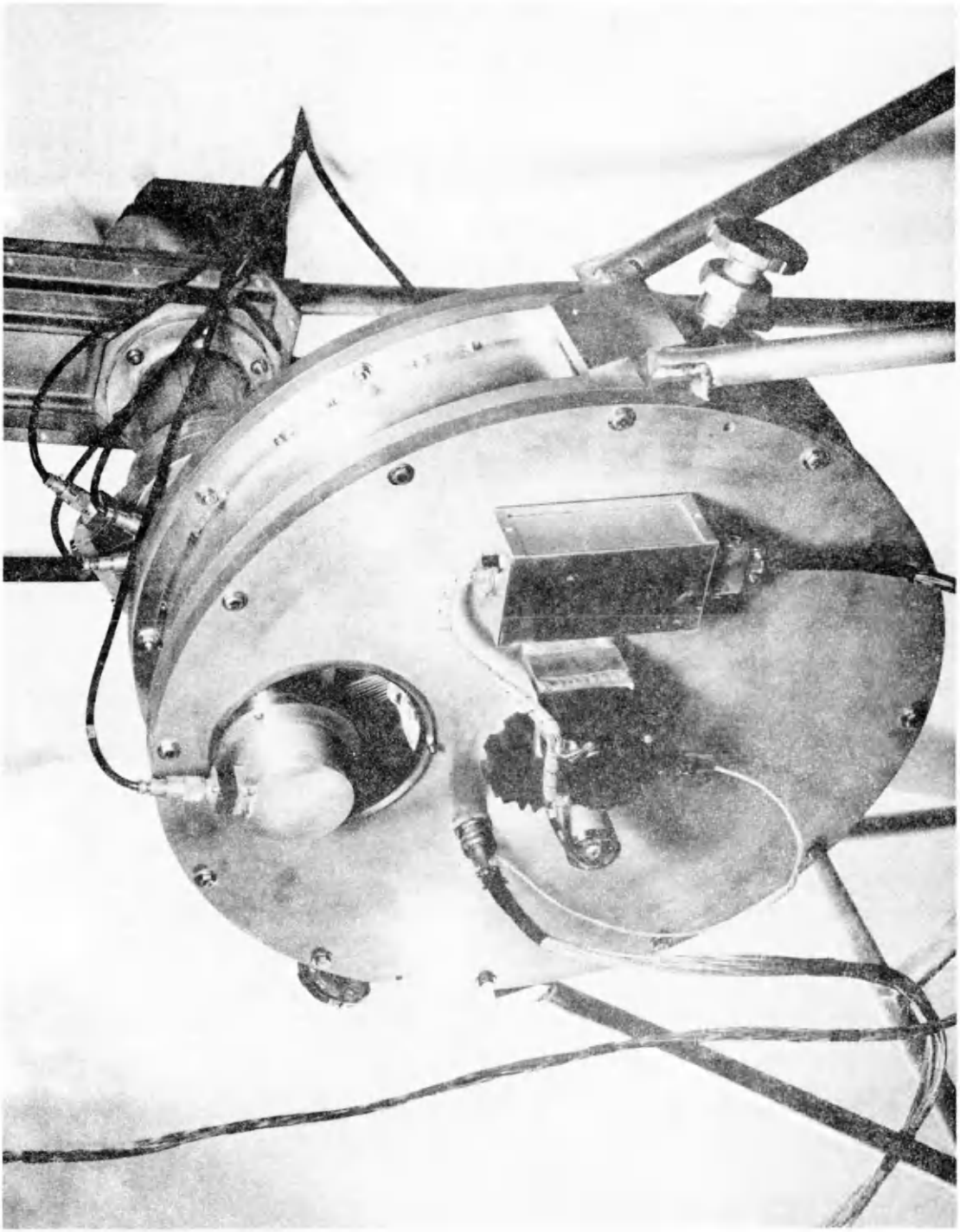

Figure 8.- Bombardment chamber connected to the 22-MeV proton beam pipe.

Proton Facilities

University of Minnesota.- The 40-MeV protons were obtained using the University of Minnesota's linear accelerator. The accelerator is capable of producing a time-averaged beam current of 10^{-8} amp. (approximately 6×10^{10} protons/sec). The cross-sectional area of the proton beam is approximately 1.25 inch^2. This area was determined by exposure of photographic film to the proton beam.

Oak Ridge National Laboratory.- The 22-MeV protons were obtained by using the 86-inch cyclotron at the Oak Ridge National Laboratory in Oak Ridge, Tenn. The 86-inch cyclotron has a fixed frequency of 13.4 mc and a magnetic field of approximately 9000 gauss. The cyclotron developes a maximum internal beam current of 3000 μa at 17.5-MeV and 1500 μa at 21-MeV. The size of the proton beam was approximately 1.25 inches in diameter. A flux rate on the order of 2×10^9 protons/sec was obtained.

Measurements During Irradiation

Temperature.- The temperature was monitored during irradiation by using a potentiometer-type pyrometer and a copper-constantan thermocouple. The temperature of the samples was maintained at 28° C $\pm$ 2° C throughout the test.

Short circuit current.- According to the formula developed in the theory, the diffusion length and lifetime can be calculated and the changes due to radiation by measuring the changes in the short circuit current generated in the base of a P-N junction. This current should be generated by a monochromatic wavelength of light in the near-infrared region.

A piece of equipment was developed to fulfill the preceeding conditions. The apparatus will be referred to as the diffusion length analyzer or analyzer. The analyzer and associated equipment are shown in figures 9 and 10. A diagram of the optical system enclosed in the analyzer is given in figure 11. It is essentially a monocromatic infrared light source constructed in four main sections, each made from 1/8-inch thick aluminum to minimize radiation darkening of optical components. A view of each section is shown in figure 9. Section 1 houses the lamp and is provided with a fan for cooling. The lamp used in the experiment was a commercial tungsten photospot lamp. Sections 2, 3, and 4 house the lenses and filters. These sections are circular tubes 4 inches in diameter and 1 foot long. The sections are threaded and allow several combinations to be used according to length desired (from 2 to 4 feet) or intensity of light desired on the samples. These combinations are beneficial in that the variation allows a certain amount of maneuverability in cramped quarters. Part 5 is an example of a brass holder used to hold lenses and filters inside the tubing. The holder is trimmed with heavy felt to reduce light leakage. The two sample holders are labeled 6 and are constructed of bronze with 1/4-inch copper tubing attached to permit water cooling. These holders are used when making measurements in the lab. Terminals are provided for current readout of the samples.

The optical lenses enclosed in the tubing of the analyzer were used to focus the light so that higher currents could be obtained, increasing the accuracy of the measurement. The light beam was regulated between 2.0 and 4.0 inches in diameter, and found to be sufficiently uniform throughout the investigation.

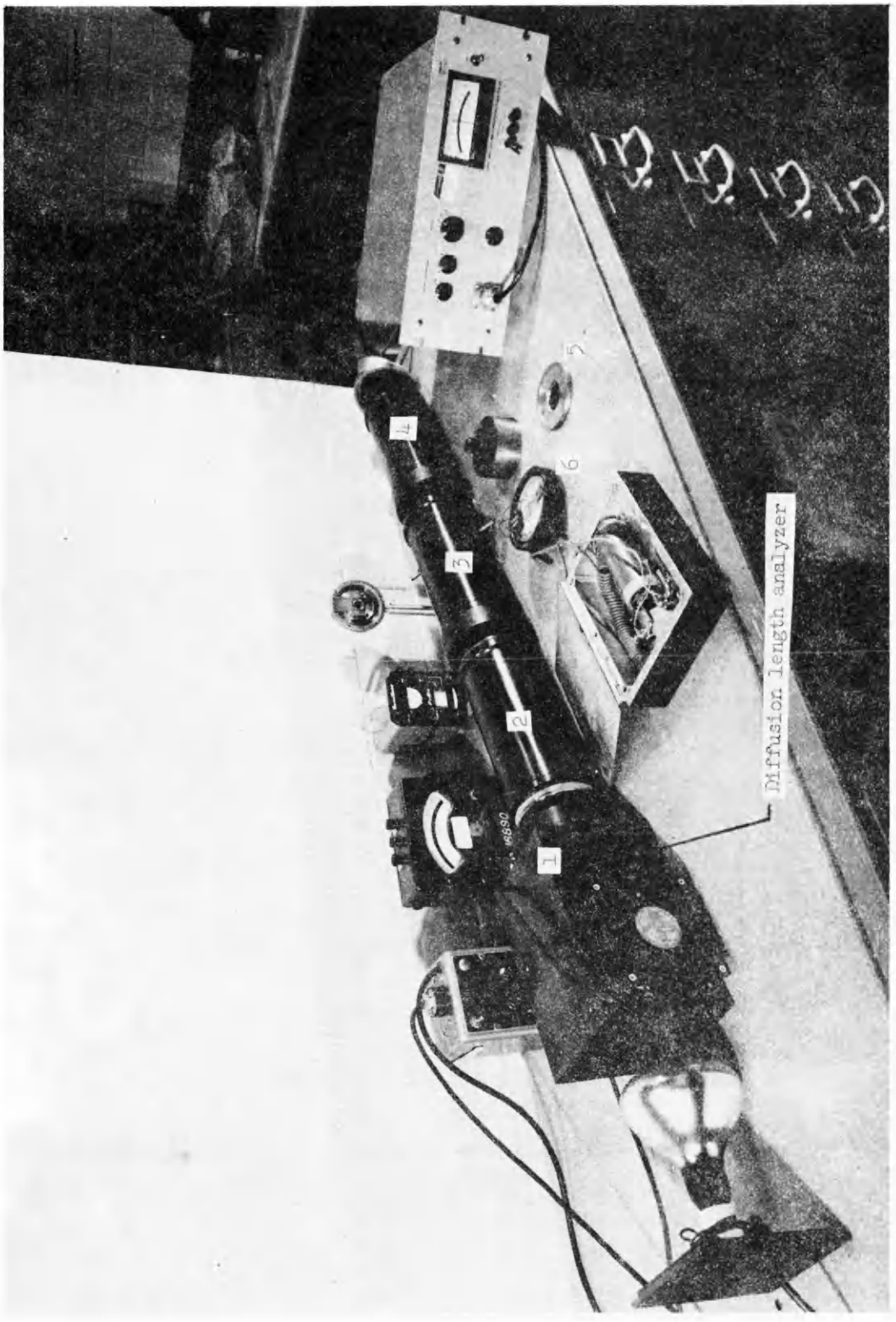

Figure 9.- Equipment for determining the diffusion length.

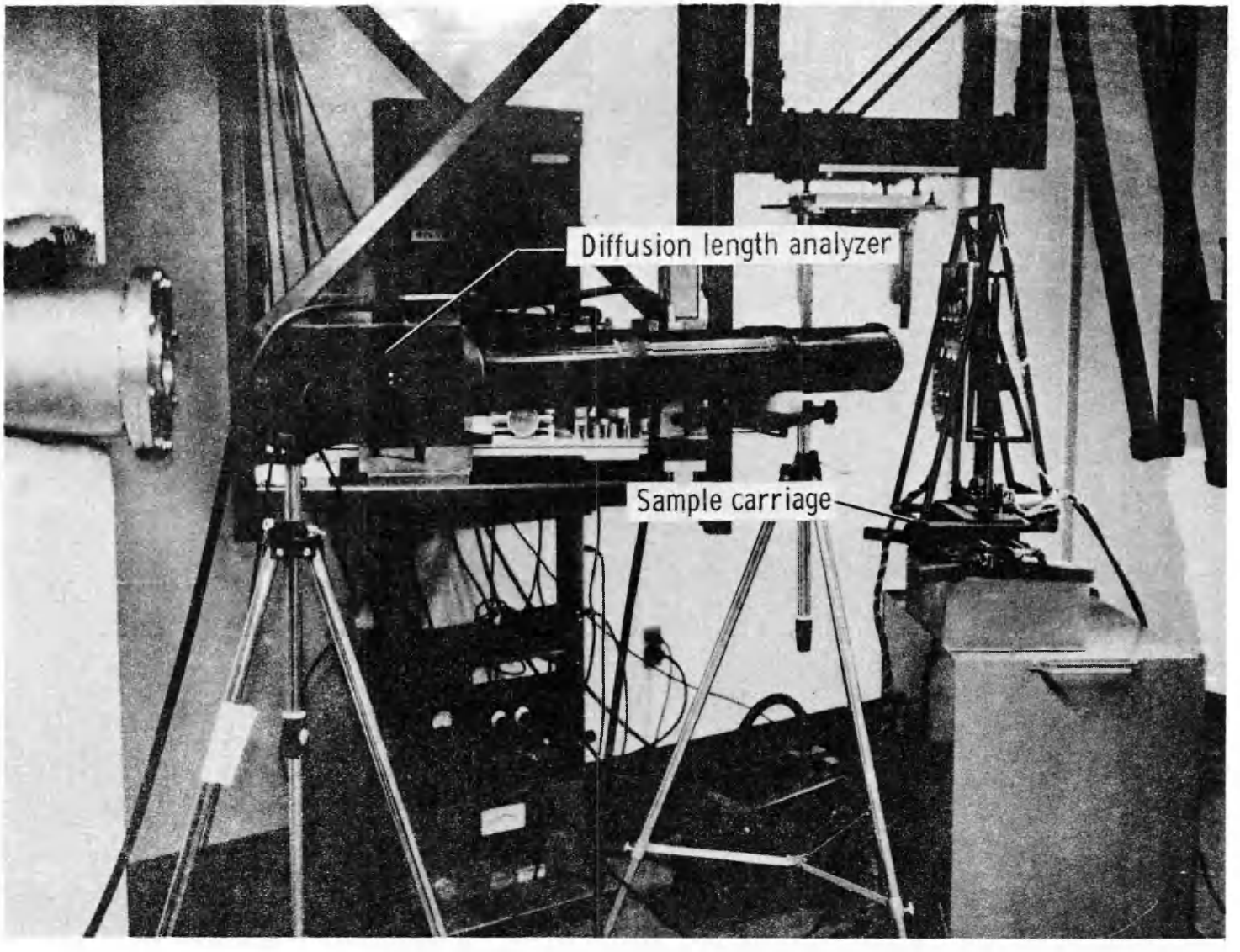

Figure 10.- Typical inbeam setup.

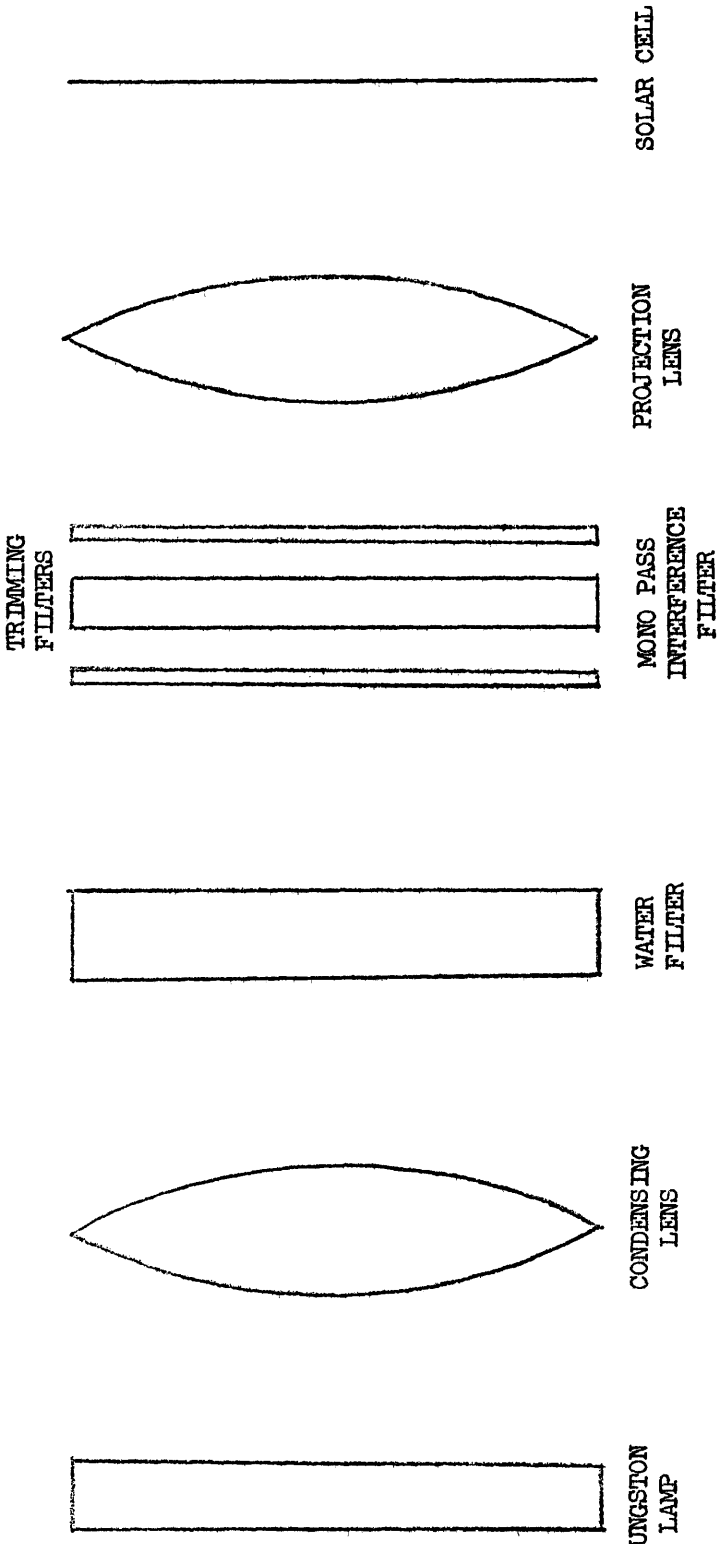

Figure 11.- Optical diagram for diffusion length analyzer.

Infrared narrow-band interference filters with nominal peak transmissions of 36 percent at 1.0 micron and 0.8 micron are provided. Transmission through the filters was measured on spectrophotometers having a range of 0.3μ and 16.0μ. It was found that the half-band width was approximately 0.025μ, and that the total transmission outside the transmission band was less than 0.10 percent. The infrared filters may be interchanged or removed completely from the system if desired.

The analyzer is connected to a voltage regulator to operate the tungsten lamp at various color temperatures. A constant voltage transformer is connected between the main power supply and the voltage regulator in order to keep a constant voltage at the lamp. The lamp voltage is monitored with a voltmeter. A milli-micro voltmeter is used to read the voltage drop across a precision 1.0 Ω resistor in series with the junction. A thermopile measured the photon flux passing through the narrow-band filter and incident on the samples. With this setup, the short circuit current and its changes due to irradiation of the samples is measured, and can be used to determine the diffusion length and lifetime of the minority carriers in a bulk semiconductor by using equation (44). This current was measured at various integrated proton fluxes by stopping the beam and turning on the analyzer. The intensity of the lamp was found to remain constant throughout the tests at approximately 100 $\mu w/cm^2$.

Integrated proton flux.- The proton flux striking the Si and GaAs samples was monitored by the use of an ion chamber using air as the gas. The output of the ion chamber was calibrated against the

results of several iron foil activation analysis measurements at the Oak Ridge National Laboratory.

At the University of Minnesota, the activation analysis method was not available. Therefore, the ion chamber was calibrated against a Faraday cup. The Faraday cup is one of the simplest methods used for determining the intensity of radiation particles. It consists essentially of a thick metal plate which will completely stop the beam. The plate has electrical connections to an ammeter so that the current generated in the plate by the irradiation is collected. This is a measure of incident charge from the radiation particles, and is measured on a current integrator. The Faraday cup for low energy protons used in these experiments is evacuated in order to reduce the number of secondary emissions. The evacuated cup had a potential of a few hundred volts in order to supress these secondary emissions electrostatically. Also the length of the cup is large compared to the diameter of the entrance aperature so that there is a small solid angle for escape of the secondary electrons. The cup was constructed of brass. It was found that the flux rate used at the University of Minnesota was 10^{10} protons/sec.

Method of making a current-flux run.- The general procedure for making a run of current versus accumulated proton flux is the same for both accelerator facilities. Both had a gate or shutter to stop the proton beam at will without cutting the machine off. This gate is closed for machine tuneup with the current reading taken off the metal gate. When this current is of the required value, the gate is opened, allowing the proton beam to pass through the ion chamber and strike the sample. The current collected by the ion chamber is electronically

read on the current integrator, and when the integrator gives the desired integrated proton flux reading, the gate is closed cutting off the beam flow, and the analyzer turned on giving a current reading in the sample. The analyzer is placed in an advantageous position beside the beam pipe. The readout system is connected by cable to a remote readout room. Figure 12 gives a block diagram of the complete inbeam setup. After the reading is recorded, the gate is opened again for another dose of protons. This cycle is repeated until the sample has been throughly observed and damaged to the desired degree. The points at which the proton beam was stopped and the current measurements taken varied according to sample behavior.

Measurements Before and Subsequent to Irradiation

Short circuit current.- The short circuit current of the samples tested were measured before irradiation in the lab by using the diffusion length analyzer. This measurement was made again just prior to irradiation, to insure that the initial conditions are the same at the test site as they were in the lab. Subsequent to the final irradiation of a particular sample, the current is measured without going through the remote system as a further check of the systems accuracy.

Temperature.- The temperature of the samples was checked using the thermocouple-pyrometer system throughout all measurements and room temperature maintained.

Reflectivity.- The reflectivity (R) of the samples was measured using a spectrophotometer. The silicon samples were measured at 1.0μ while the GaAs samples were checked at 0.8μ and 0.9μ. The samples were measured again after irradiation to determine any changes in the reflectance due to radiation damage. There were no changes observed.

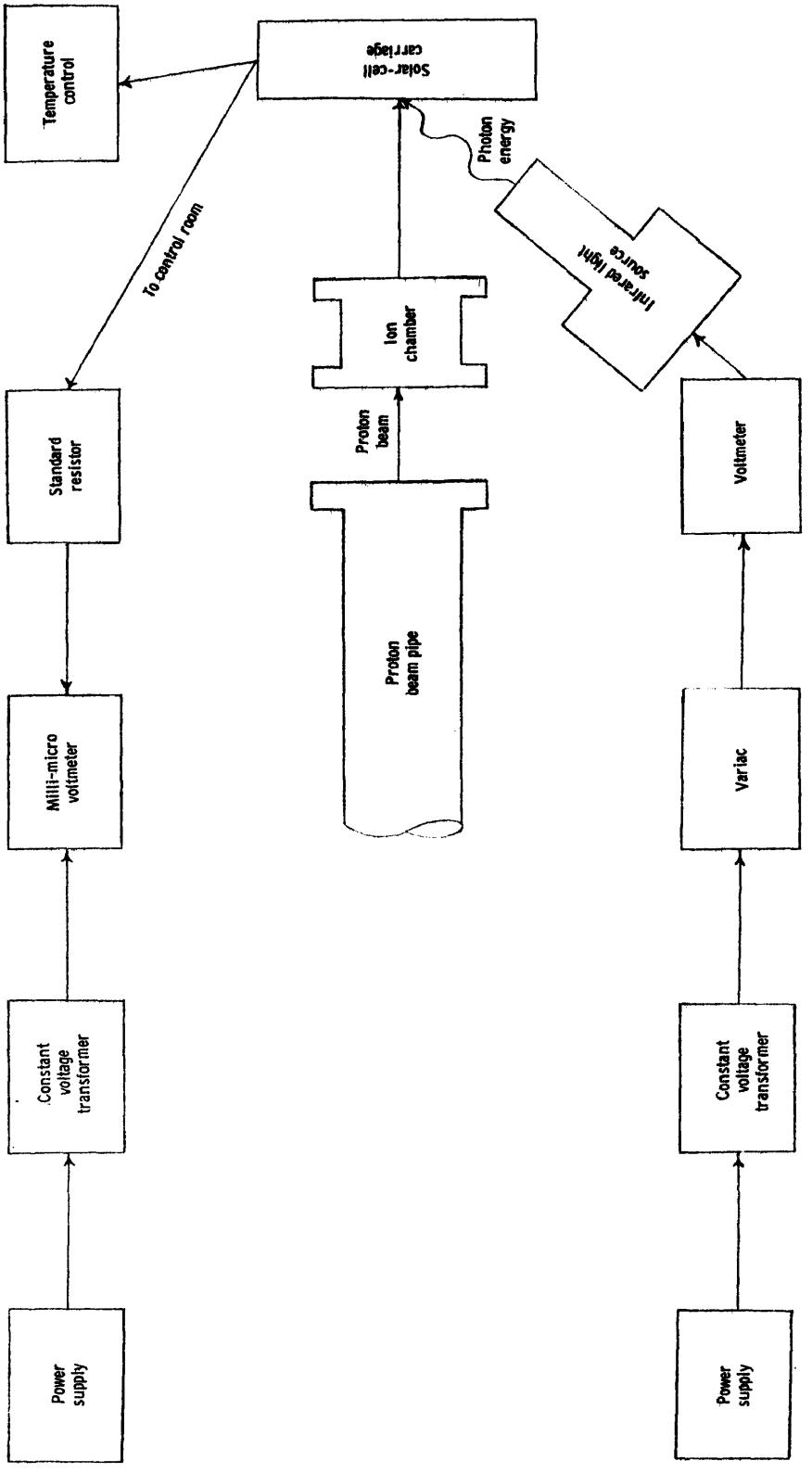

Figure 12.- Block diagram of readout system used in inbeam measurements.

CHAPTER IV

EXPERIMENTAL RESULTS

22-MeV Protons

Silicon.- There exists a large difference in the reduction of minority carrier lifetime in N- and P-type silicon for 22-MeV proton bombardment. Figure 13 is a typical plot of the lifetime at a particular flux divided by the initial lifetime before radiation for N-type silicon. The same type of typical plot for P-type silicon is given in figure 14 (The accuracy of the points shown on all the curves in this report are within ± 5.0 percent). The samples were irradiated using a constant intensity and energy proton beam. The curves showing the results of this bombardment are plotted on log-linear coordinate paper and show a steep straight line section having an approximately constant negative slope bending to an almost horizontal section. Both sets of plots depict a rapid and uniform introduction of damage centers. The rapidity of the production of radiation induced defect centers can be seen by observing the swift reduction in lifetime at low proton fluxes. For all practical purposes the material is destroyed at integrated proton fluxes from 10^{11} protons/cm^2 on. The lifetimes are so low in this area that no practical application of the material could expect to be attained. This means that any electronic device constructed of either N- or P-type silicon which would experience 22-MeV proton fluxes ± ~ 5-MeV would experience failure in the high 10^{11} protons/cm^2 range.

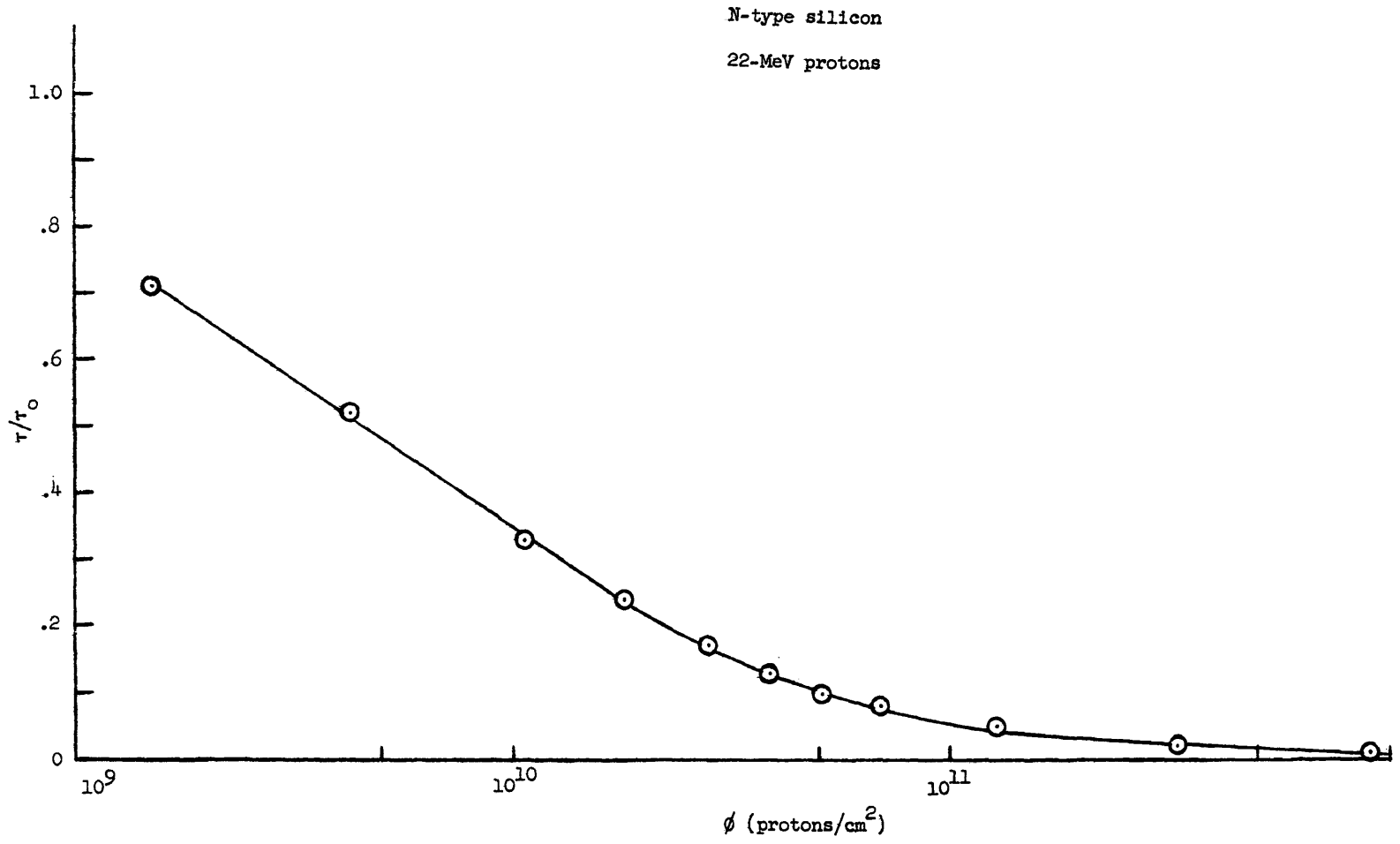

Figure 13.- Typical curve for integrated flux versus percent change in hole lifetime for N-type silicon irradiated with 22-MeV protons.

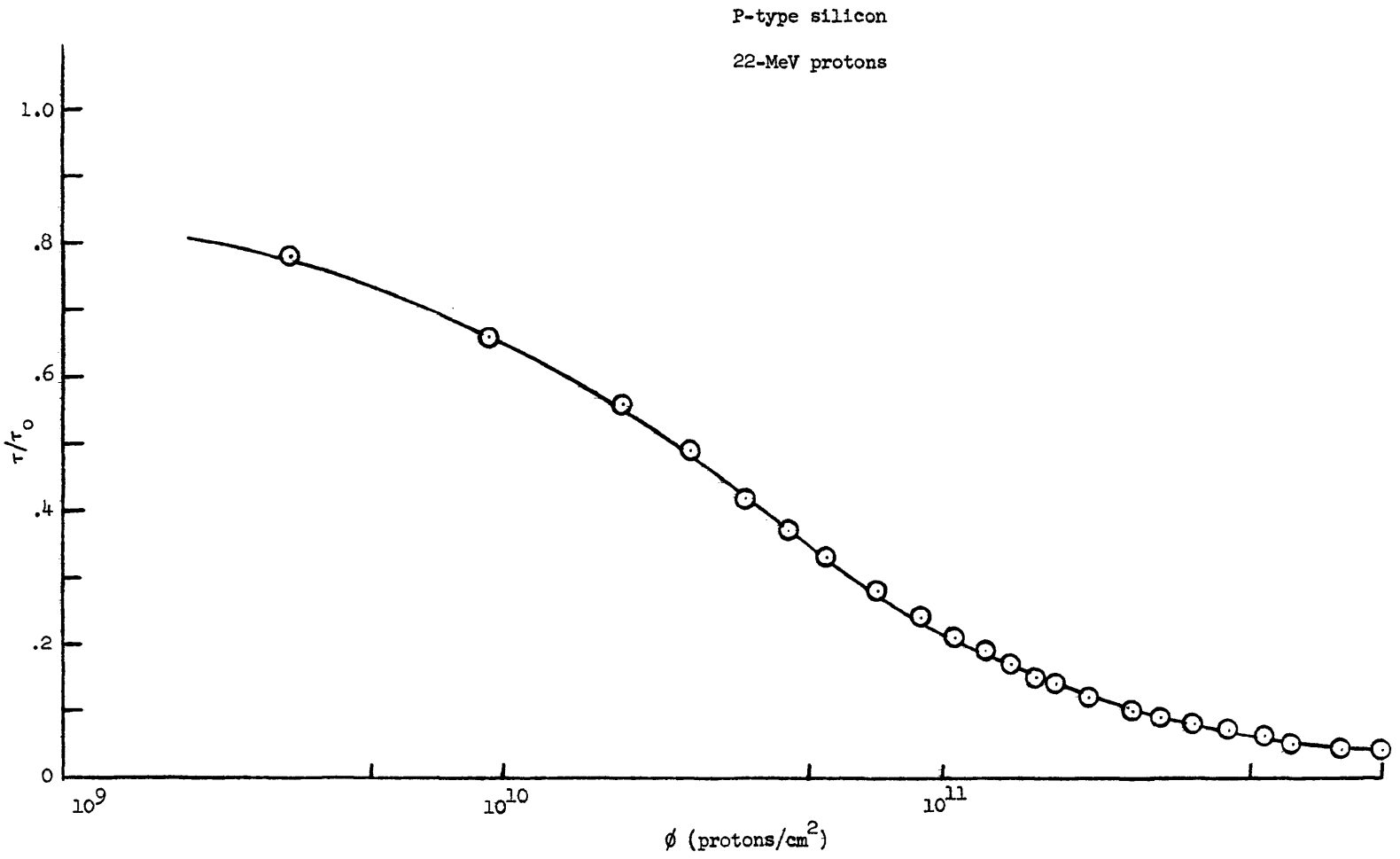

Figure 14.- Typical curve for integrated flux versus percent change in electron lifetime for P-type silicon irradiated with 22-MeV protons.

There is, however, a large difference between P- and N-type silicon at the same total integrated fluxes. P-type silicon is much less damaged by the protons than is N-type silicon. P-type silicon has a reduction rate of the lifetime of approximately 2 1/2 times less than N-type silicon compared to their initial values, this is true within the integrated proton flux range of 10^9 - 10^{11} protons/cm^2. From 10^{11} protons/cm^2 and higher there is a saturation effect caused by the large number of defect centers produced. This means that due to the great magnitude of centers uniformly oriented within the crystal, the free minority carriers produced by thermal, photon generation, or any other excitation are quickly captured by the defect centers, and therefore, have a very short lifetime.

The uniformity of the production of defect centers can be assumed since the damage slope from sample to sample is the same with no gross deviations.

Gallium arsenide.- Figures 15 to 17 give the damage from 22-MeV protons to the minority carrier lifetime in P-type gallium arsenide in plots of the same nature as was used for silicon. The plots begin with 10^{12} protons/cm^2 since there is less than 20 percent reduction in the lifetime for total fluxes up to this point. This means that gallium arsenide has its initial lifetime reduced by less than 20 percent at total integrated fluxes where silicon of both types have experienced a reduction in minority carrier lifetime by more than 90 percent. It would appear then that gallium arsenide would be far superior to silicon in a radiation environment, and this may be the case, but, there are several points to consider before making this statement. First, the initial lifetime of gallium arsenide is on the

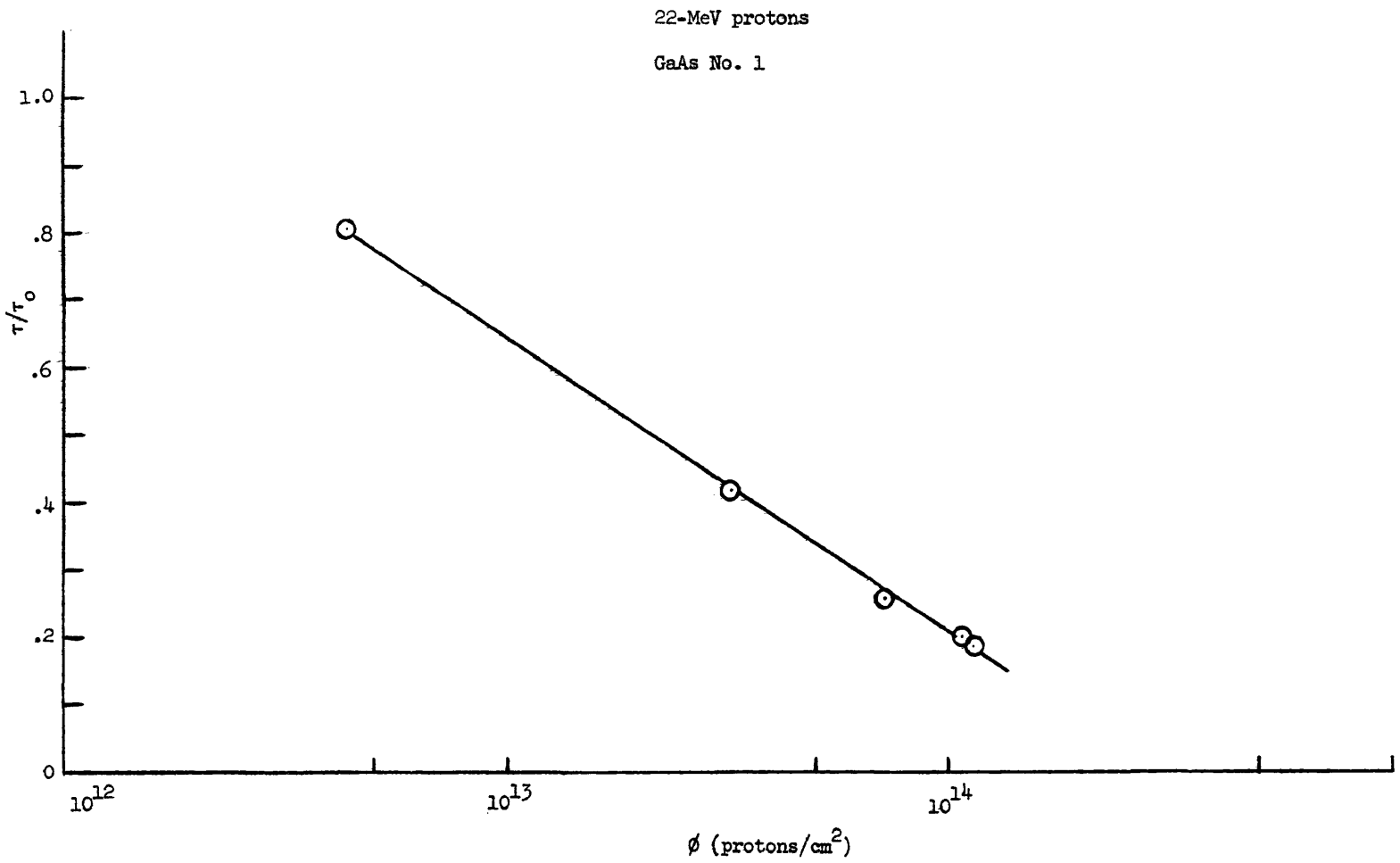

Figure 15.- Percent change of hole lifetime versus integrated flux for N-type gallium arsenide irradiated with 22-MeV protons. (Sample No. 1).

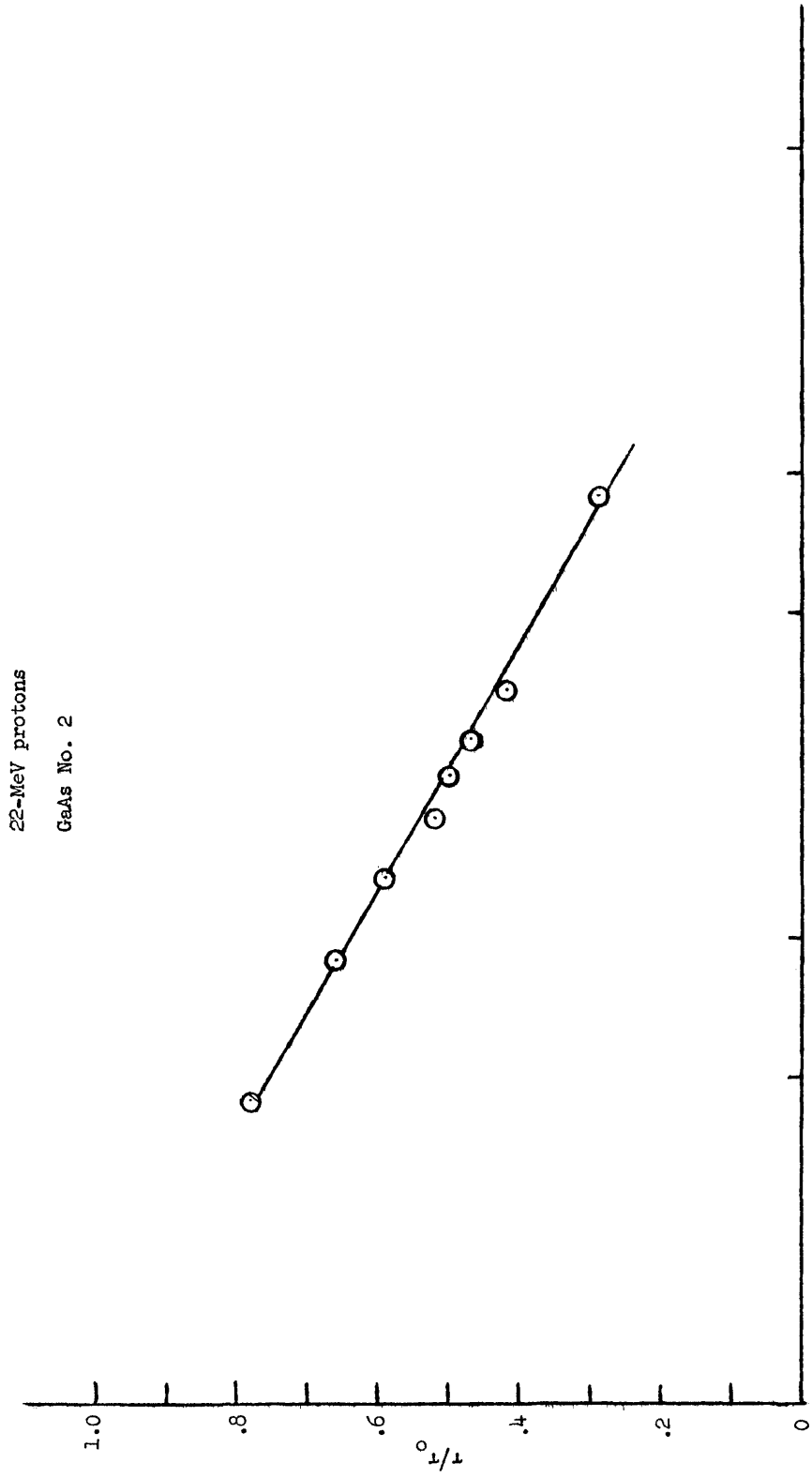

Figure 16.- Percent change of hole lifetime versus integrated flux for N-type gallium arsenide irradiated with 22-MeV protons. (Sample No. 2).

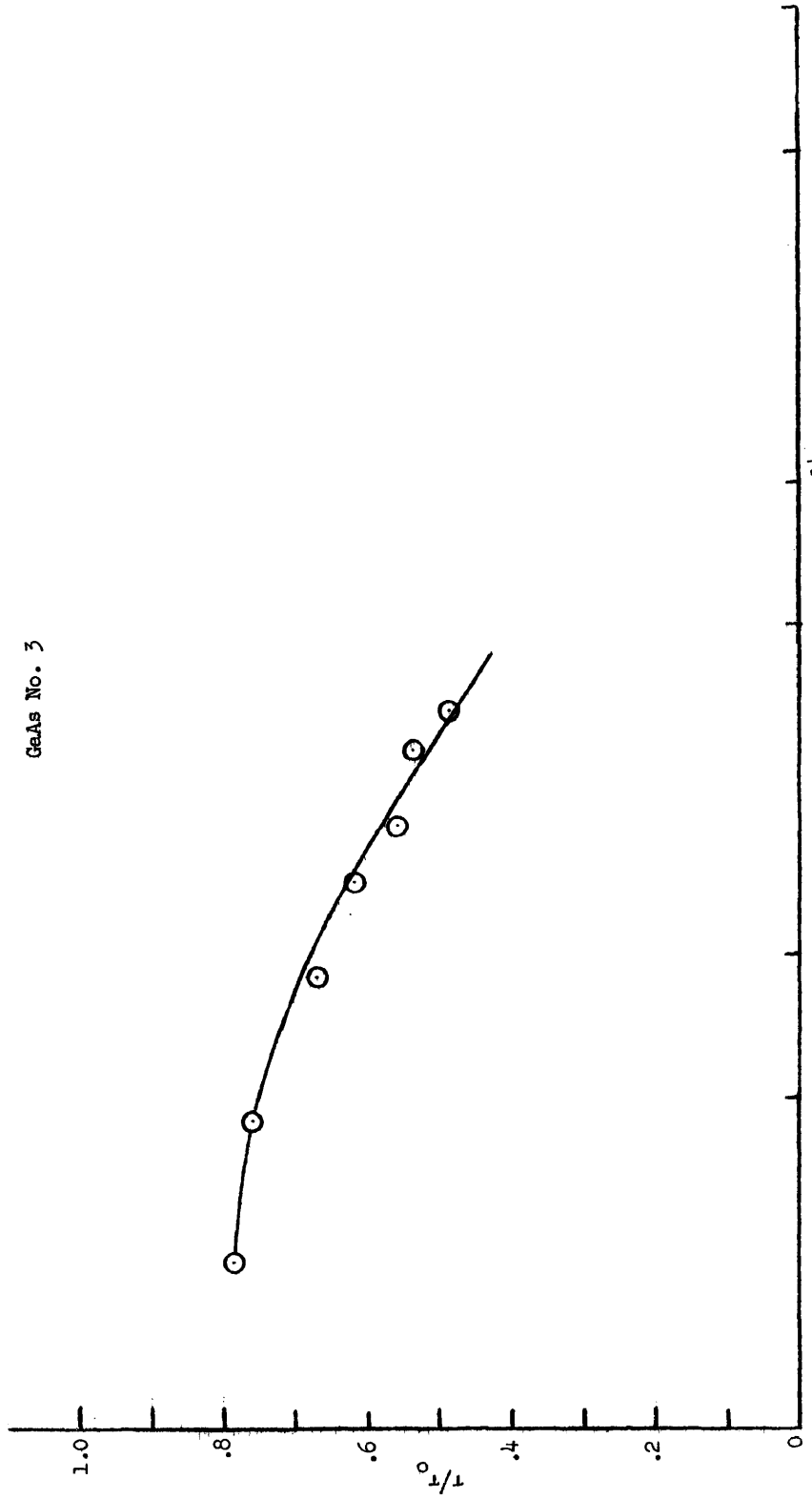

Figure 17.- Percent change of hole lifetime versus integrated flux for N-type gallium arsenide irradiated with 22-MeV protons. (Sample No. 3).

order of nanoseconds while for silicon it is in the microsecond range. But, the minority carrier lifetime in gallium arsenide is being increased due to better methods of fabrication, and it is expected to be increased until the material will be competitive with silicon. When this is done the reduction rate in the lifetime may increase, since obviously more carriers are being generated, and damage produced defects could capture the added carriers causing them to recombine at a more rapid rate than now experienced.

Second, it can be seen from the figures that at a total integrated flux of around 5×10^{12} protons/cm^2 for 22-MeV protons the lifetime begins to reduce rapidly in a slope similar to P-type silicon. Therefore, gallium arsenide is not invulnerable to high doses of radiation.

Third, there is evidence (ref. 24) that gallium arsenide is more grossly affected at its surface than in the bulk of the crystal as is silicon. This would mean that low energy protons (< 20-MeV) could possibly damage gallium arsenide more than silicon.

Fourth, the "state of the art" of gallium arsenide is not nearly as good as silicon. The crystals are harder to grow and purity is not good. Due to the complications involved in the fabrication process, gallium arsenide samples are much more expensive than silicon.

However, these statements are not intended to discredit the capabilities of gallium arsenide. Tests here have shown gallium arsenide to be far superior to silicon under radiation from 22-MeV protons which is an optimum energy in the Van Allen Belts, and it is possible that it will not degrade greatly when lifetimes are increased, or might still degrade much less than silicon. Also, the "state of the art" of gallium arsenide is improving every day.

40-MeV Protons

Silicon.- Figures 18 and 19 are the same type of typical plots used for 22-MeV protons. Again they are for both N- and P-type silicon. A similar slope of the curves exists for 40-MeV protons as 22-MeV, but the magnitude of lifetime reduction is not as great. This means that the damage cross section for 40-MeV protons is not as great as for 22-MeV protons. This is to be expected if the 1/E theory holds true for damage production. It is believed by the experimenter that the flux determination at the 40-MeV proton test was on the low side due to the fact that a Faraday cup had to be used to calibrate the ion chamber which possibly had some leakage for the current produced in it. If this is true it would mean that the damage to silicon from 40-MeV protons is even less than depicted. Even so, the lifetime is again reduced from microsecond to nanoseconds in the high 10^{11} proton/cm^2 range.

Gallium arsenide.- The same types of plots for 40-MeV damage in gallium arsenide are shown in figures 20 through 22, as were depicted for 22-MeV. The damage to gallium arsenide up to 10^{12} protons/cm^2 for 40-MeV is almost zero. Then, at about 5×10^{12} protons/cm^2 the lifetime begins to fall as rapidly as it did for 22-MeV protons. The change in lifetime in gallium arsenide is similar for irradiations with 22- and 4-MeV protons. There is a point where the GaAs crystal experiences the start of a breakdown due to the large magnitude of the accumulated proton flux. This point seems to be energy dependent (at least from 20- – 40-MeV for protons).

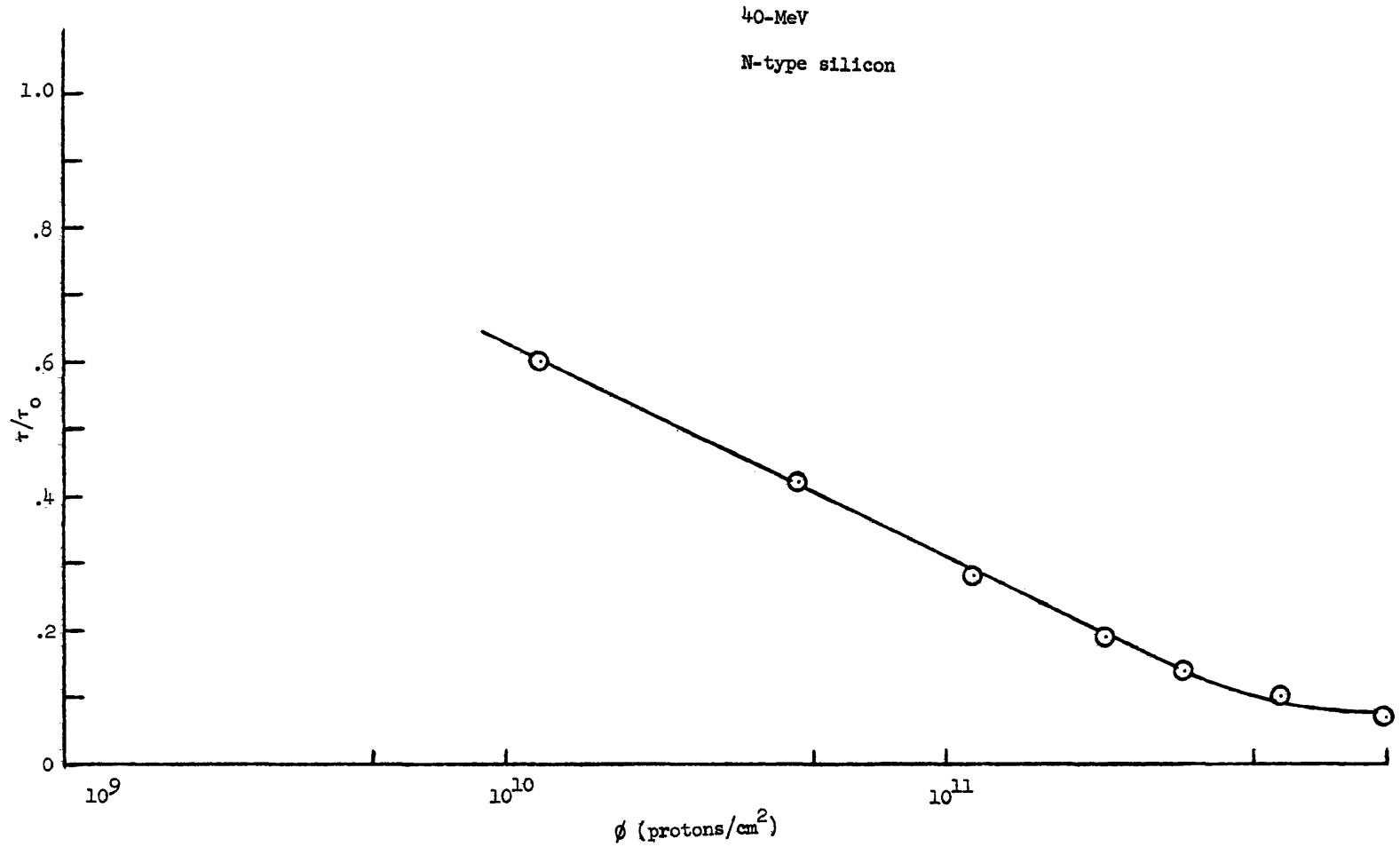

Figure 18.- Typical percent change of hole lifetime versus integrated flux for N-type silicon irradiated with 22-MeV protons.

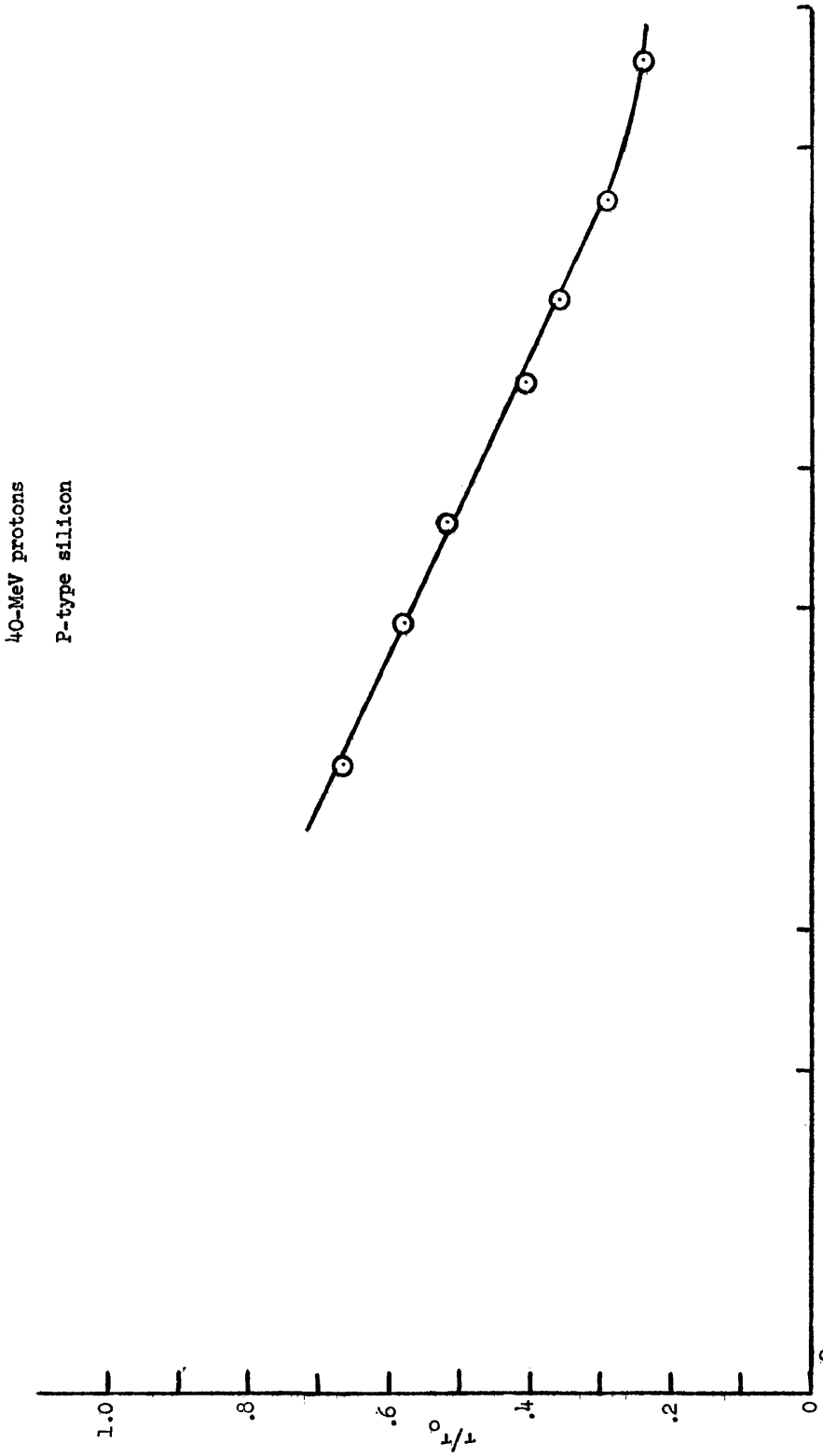

Figure 19.- Typical percent change of electron lifetime versus integrated flux for P-type silicon irradiated with 40-MeV protons.

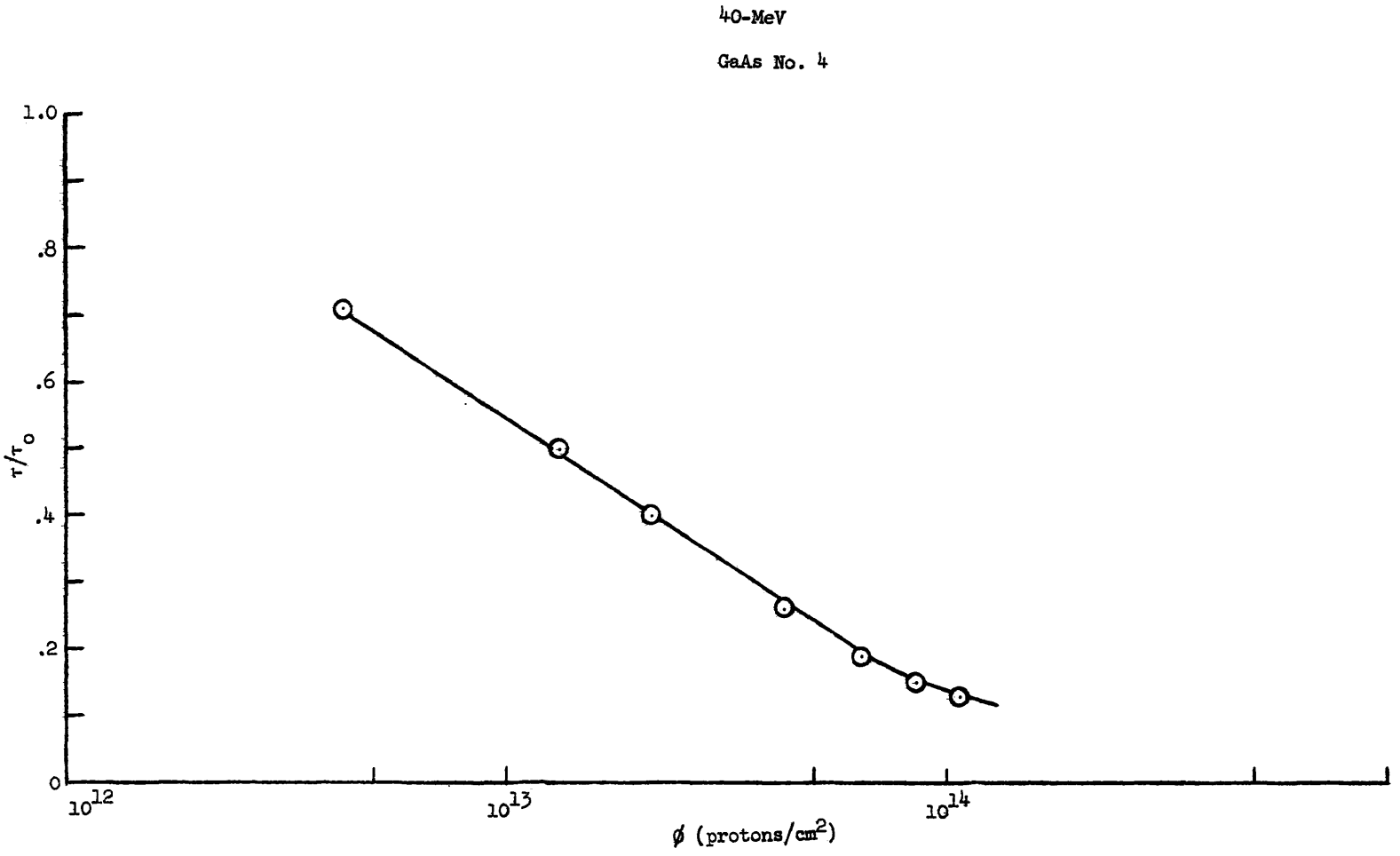

Figure 20.- Percent change of hole lifetime versus integrated flux in N-type gallium arsenide irradiated with 40-MeV protons. (Sample No. 4).

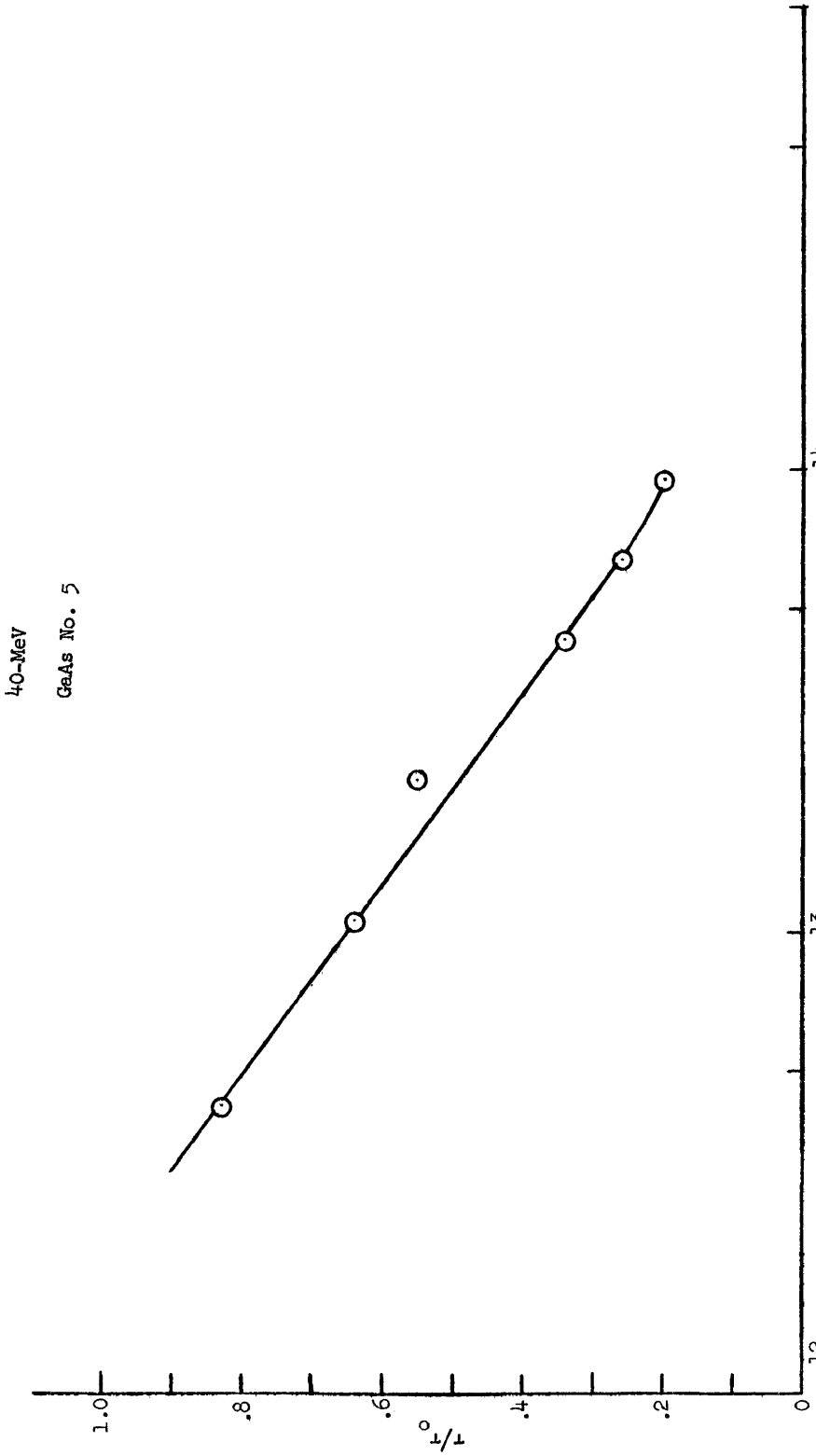

Figure 21.- Percent change of hole lifetime versus integrated proton flux in N-type gallium arsenide irradiated with 40-MeV protons. (Sample No. 5).

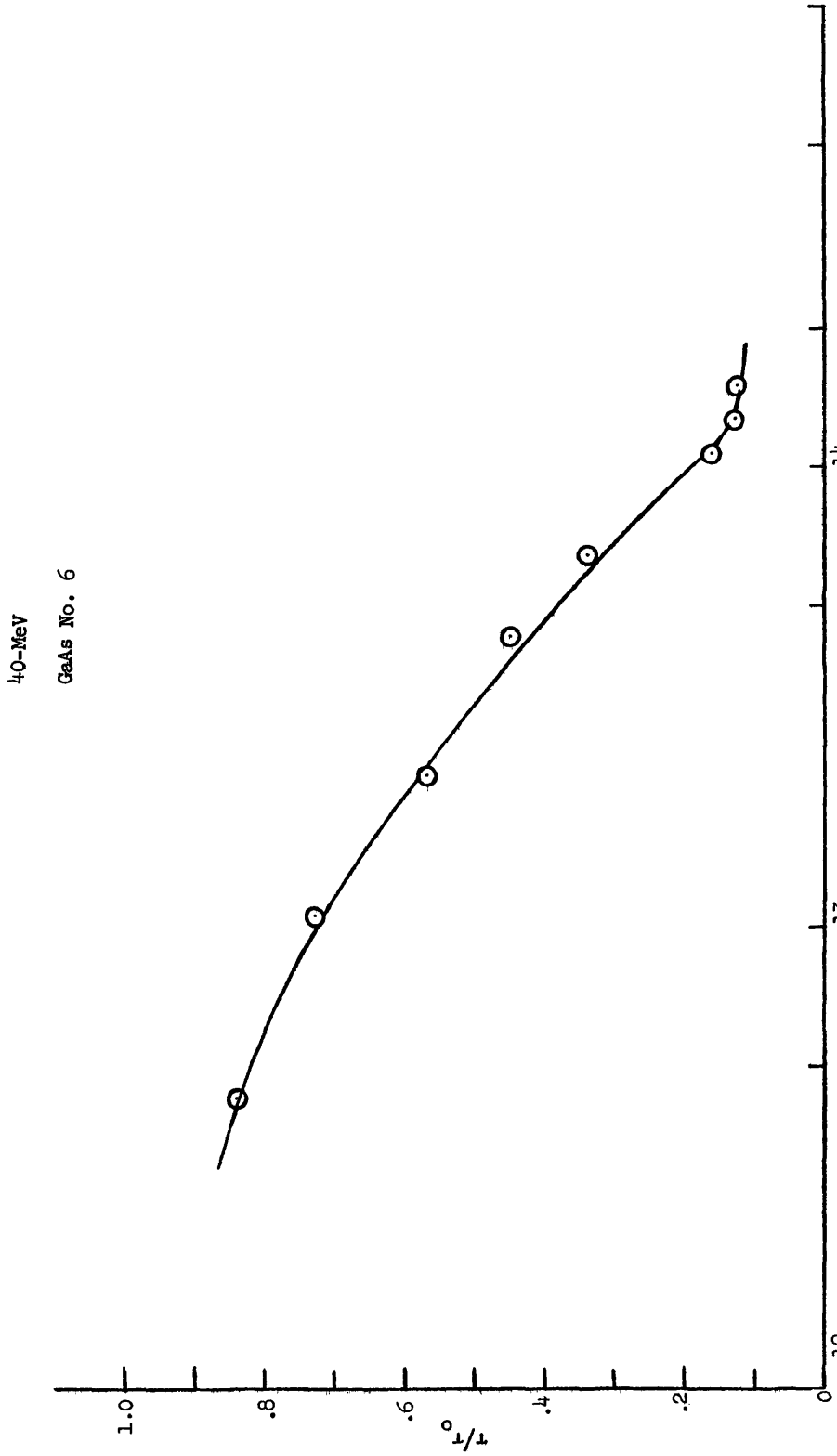

Figure 22.- Percent change of hole lifetime versus integrated proton flux in N-type gallium arsenide irradiated with 40-MeV protons. (Sample No. 6).

Comparison of 22- and 40-MeV Proton Damage

Table II will give an indication of the uniformity of the lifetime measurement as well as an indication of the uniform production of radiation defects within the particular type of crystal studied. In most cases, samples which had similar initial lifetimes were irradiated at a particular test. But, due to the difficulty of forming P-N junctions with the same initial conditions, it was not possible to keep the same lifetimes throughout all the tests as can be especially seen with P-type silicon. For the 22-MeV test the P-type silicon samples fabricated had short initial lifetimes of about 4.0 microseconds while the samples for 40-MeV protons the samples of P-type silicon had initial lifetimes on the order of 10.0 microseconds. However, from studies with N-type in which the initial lifetime varied quite largely from sample to sample and from samples of P-type with shorter initial lifetime, it was found that the damage slopes found from the ratios of lifetimes at various fluxes to the initial lifetime was the same for the same type of semiconductor material. This means that there is little difference in radiation damage to semiconductor materials of the same type with long and short lifetimes as far as the type and amount of defects produced. However, material with long lifetimes will behave better in a radiation environment, because it takes longer for the defects to capture current carriers (electrons and holes), recombine, leave, and reduce the lifetime to a point where the conductivity of the crystal would be of no practical value.

Both long and short lifetime semiconductors have saturation points which are near the same value of flux (although varying somewhat in magnitude).

From table II, it is easy to see the difference between the various types of semiconductors for 22- and 40-MeV proton irradiation. Figure 23 shows a comparison of all three types of semiconductors tested at 40-MeV using the same type of plot used throughout the text. From this plot one can ascertain that gallium arsenide experiences no reduction in carrier lifetime until a flux of about 5×10^{11} protons/cm^2 is reached where the N-type GaAs holes begin to decrease slowly in lifetime. Both types of silicon experience much more deleterious effects than gallium arsenide. The P-type silicon being affected less than N-type. It can be seen from this typical plot that the slope for N- and P-type silicon is generally the same. This would seem to indicate that the difference between damage introduction rates for the two types of silicon is an inherent one remaining constant throughout the defect center production.

Figure 24 is a typical plot for the three materials tested with 22-MeV protons. It can be seen by looking at the N-type gallium arsenide, that gallium arsenide tends to decrease slightly at low fluxes for 22-MeV protons. The decrease is still less than 20 percent for fluxes up to 1×10^{12}, but indicates that 22-MeV protons are introducing more damage in gallium arsenide than did 40-MeV protons. This is understandable since the cross-section for collision of the protons with the silicon impurity and other foreign atoms is greater. Gallium arsenide is still seen to be much less damaged by defect production than either type of silicon.

Looking at the two types of silicon we see that P-type is still far superior to N-type. Both types have minority-carrier lifetime reductions greater for 22-MeV than 40-MeV. Examples of this would

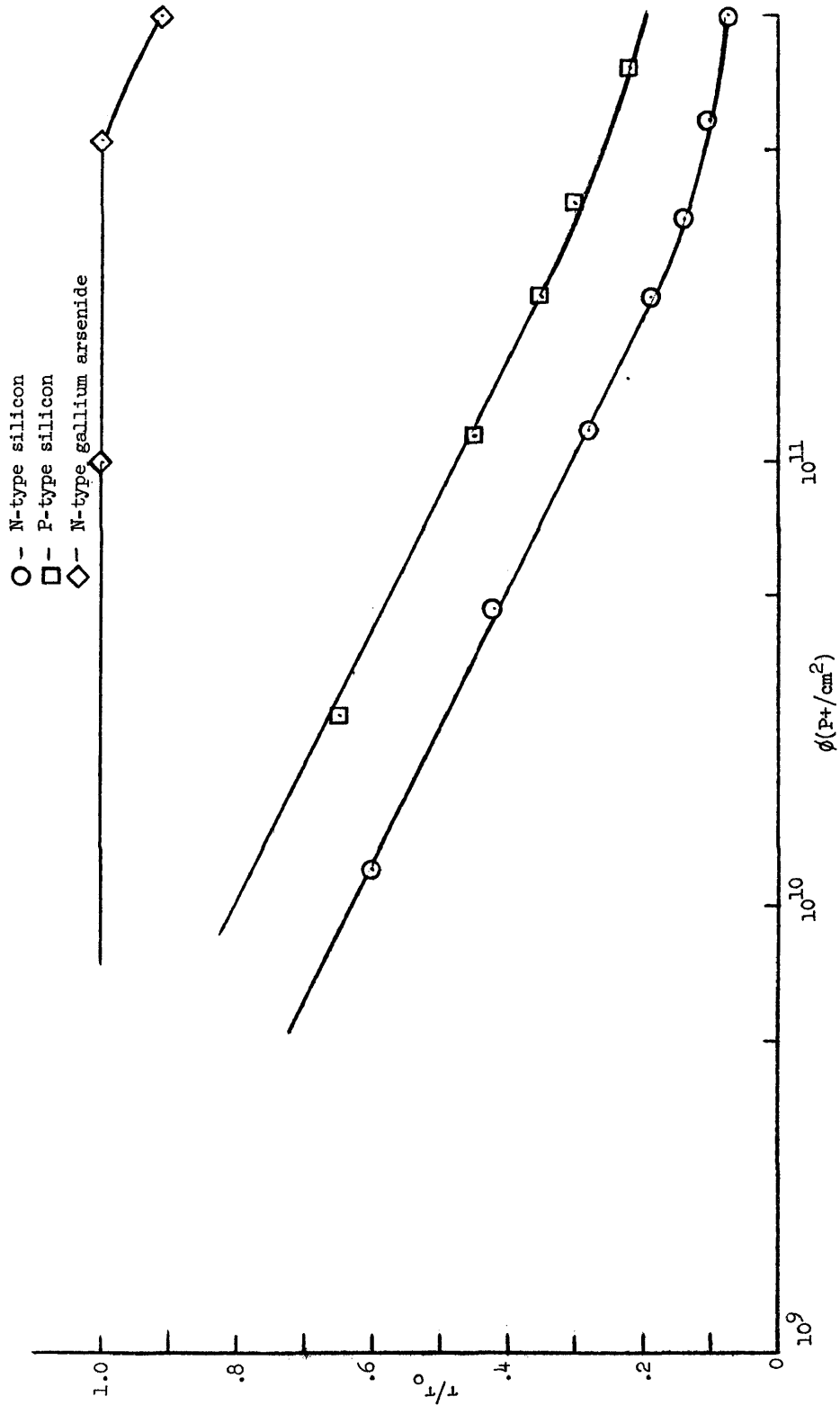

Figure 23.- Comparison of typical samples of N-type silicon, P-type silicon, and N-type gallium arsenide irradiated with 40-MeV protons.

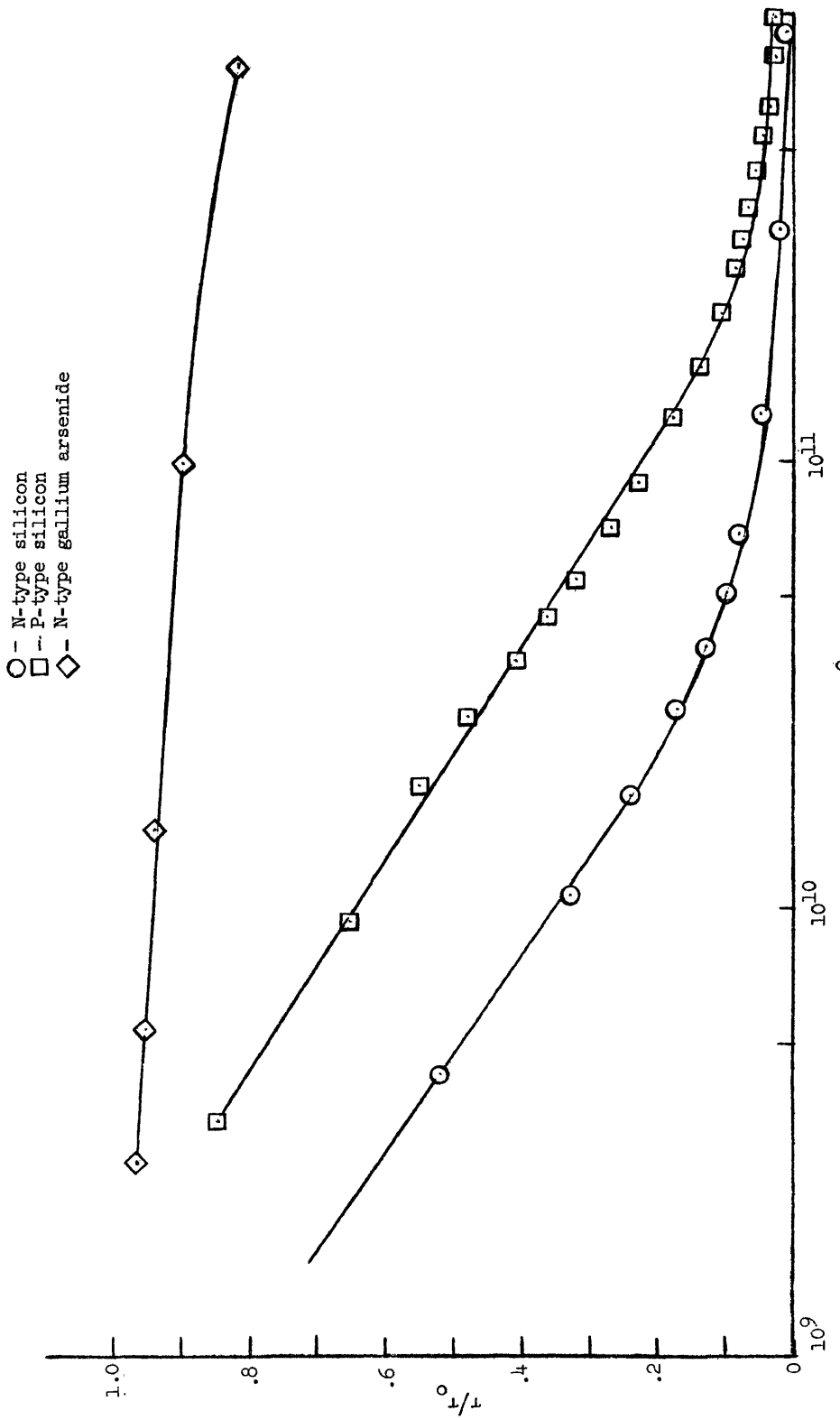

Figure 24.- Comparison of typical samples of N-type silicon, P-type silicon, and N-type gallium arsenide irradiated with 22-MeV protons.

be that for P-type silicon at 1×10^{10} protons/cm^2 the lifetime is reduced by 45 percent for 22-MeV protons, whereas it is reduced by only 20 percent for 40-MeV protons. The same measurements on N-type give 65 percent and 37 percent respectively. The difference between N-type and P-type silicon is greater for 22-MeV protons than 40-MeV. This means that P-type silicon will withstand a more severe radiation environment than N-type silicon.

Between $2\text{-}3 \times 10^{11}$ protons/cm^2 for 22-MeV, there is a difference in slope between P- and N-type silicon not observed at 40-MeV. This is probably due to the fact that the damage becomes so large and complex at these high integrated fluxes for 22-MeV protons that a saturation of damage centers is achieved more quickly in the rapidly decreasing N-type silicon. It should be noticed also that due to the increase in damage centers produced in both types by 22-MeV protons, the difference between the two types is much less at low energy protons than high energy.

Gallium arsenide was the main material of interest and seemed to be much more radiation resistant than silicon, the samples were irradiated to very high integrated fluxes in the 10^{14} protons/cm^2 range. The results of this study are shown in figure 25. It can be seen that gallium arsenide does degrade in carrier lifetime at very high proton fluxes, dropping to approximately 20 percent of the initial lifetime at a flux of 1×10^{14} protons/cm^2. The slope of the damage curve seems to be the same for both 22- and 40-MeV protons. When gallium arsenide does begin to degrade rapidly at around 1×10^{13} protons/cm^2, it seems to have a damage slope almost identical to P-type silicon for 22-MeV irradiation. The silicon slope begins at about 5×10^9 protons/cm^2, however.

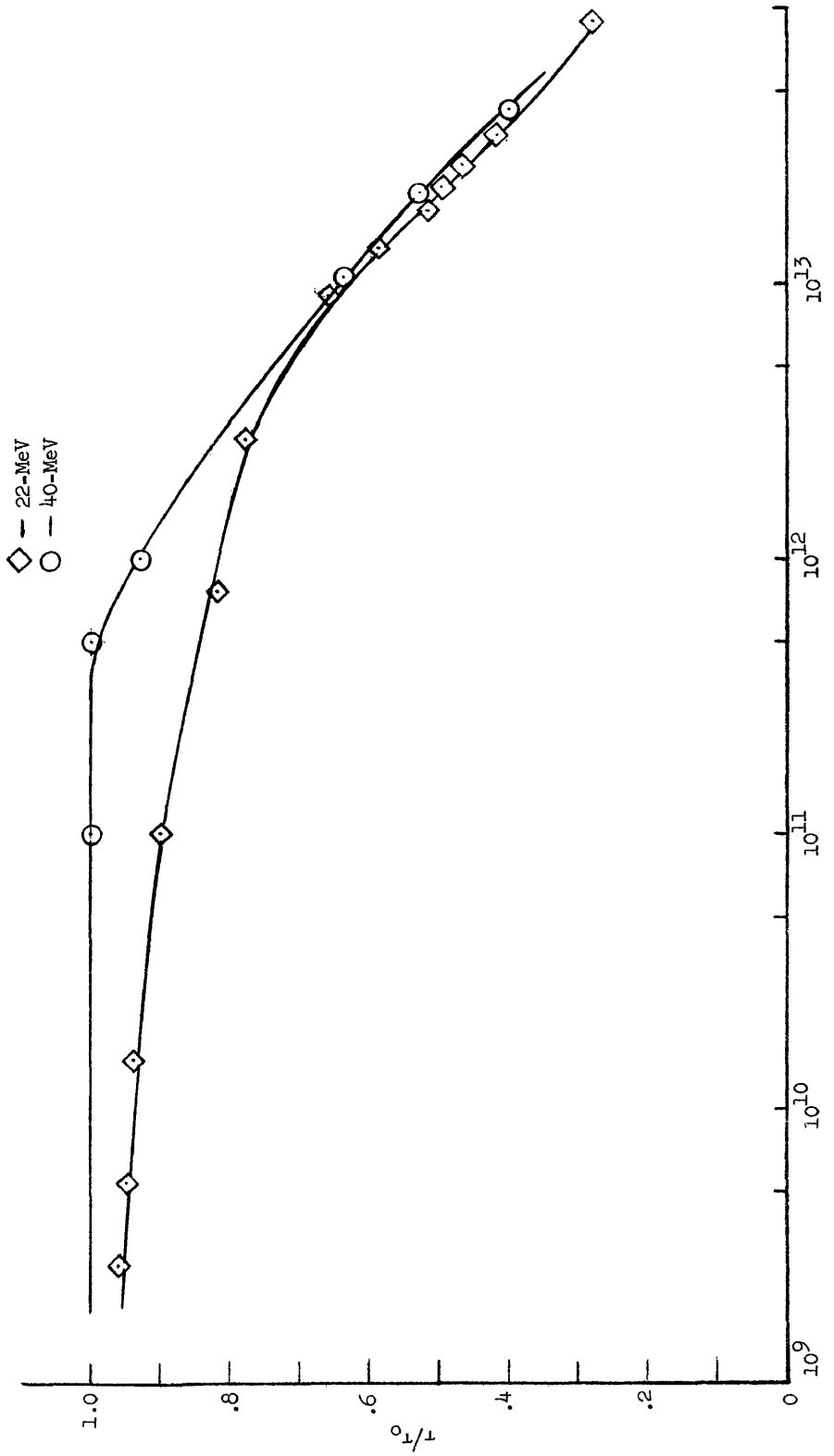

Figure 25.- Comparison of samples of N-type gallium arsenide from 22- and 40-MeV proton irradiation.

For all practical purposes, gallium arsenide may still be considered as being only slightly affected by radiation damage since integrated proton fluxes in the 10^{13} - 10^{14} proton/cm^2 range are not usually received by space vehicles in the normal lifespan of the vehicle operation.

CHAPTER V

CONCLUSIONS

The difference in radiation damage between silicon and gallium arsenide can be interpreted in terms of minority carrier lifetime. In terms of photon-generated current carriers, the majority of the carriers are located deep in the crystal for silicon and close to the surface for gallium arsenide as a result of the absorption process. This could mean that gallium arsenide would be more severely damaged by low energy protons than silicon.

The primary damage mechanisms produced in semiconductors is the introduction of lattice displacements (vacancies and interstitials). From data presented here it appears that N-type gallium arsenide is superior to both N- and P-type silicon in radiation resistance to 22- and 40-MeV proton bombardment. This superiority can be attributed to two main effects:

1. Gallium arsenide is a semiconductor material having very short minority carrier lifetimes. Devices made with this material are designed in such a way that the efficiency of the operation is not affected by the short lifetimes or changes in the lifetime to a great degree.

2. The atomic weight of both gallium and arsenic used to form the compound gallium arsenide is 2 1/2 times heavier than silicon

atoms. This means that the threshold energy (the energy required to move an atom out of its normal position within the crystal lattice) is much greater for gallium arsenide than for silicon. This has the effect of lowering the overall general level of damage in gallium arsenide.

The 1/E damage theory holds true for proton irradiation of silicon for energies of 22- and 40-MeV. In GaAs the 22-MeV protons are more damaging at low fluxes than 40-MeV, but the damage seems to equalize at higher fluxes.

The GaAs damage mechanism could be formation of a silicon-vacancy or a donor-vacancy, since silicon, Cu, Cr, and Ca are the largest impurities.

The results obtained from the technique were very satisfactory and shows the method has the possibility of being used with more complicated experiments to help determine more about the radiation damage mechanism in semiconductors.

The results tend to back the theory that GaAs is a better semiconductor material to use in a radiation environment.

REFERENCES

1. Brown, W. L.; Augustyniak, W. M.; and Waite, T. R.: J. Appl. Phys. 30, 1195 (1959).
2. Watkins, G. D.: J. Phys. Soc. Japan 18, 22 (1963).
3. Wertheim, G. K.; and Buchanan, D. N. E.: J. Appl. Phys. 30, 1232 (1959).
4. Baicker, J. A.: Phys. Rev. 129, 1174 (1963).
5. Wertheim, G. K.: Phys. Rev. 110, 1272 (1958).
6. Rosenzweig, W.; Smits, F. M.; and Brown, W. L.: J. Appl. Phys. 35, 2707 (1964).
7. Oliver, J. W.: Space Technology Lab. Inc., MR-16 (8987-0001-RU-001), February 19, 1962.
8. Rosenzweig, W.: Bell Sys. Tech. J. XL1, 1573 (1962).
9. Lark-Horovitz, K.: Nucleon Irradiated Semiconductors, Symposium Volume of the Reading Conference (London, Butterworth's Publishing Co., 1951).
10. Bemski, G.: J. Appl. Phys. 30, 1195 (1959).
11. Watkins, G. D.; Corbett, J. W.; and Walker, R. M.: J. Appl. Phys. 30, 1198 (1959).
12. Watkins, G. D.; Corbett, J. W.: Phys. Rev. 121, 1001 (1961).
13. Watkins, G. D.; and Corbett, J. W.: General disucssions of Faraday Society, Paris, 1961.

14. Arnold, D. M.: et. al., National Aeronautics and Space Administration, NASA CR-40, April, 1964.

15. Shockley, W.; and Read, W. T.: Phys. Rev. 87, 835 (1952).

16. Loferski, J. J.; and Rappaport, P.: Phys. Rev. 111 No. 2, 432 (1958).

17. Hall, R. N.: Phys. Rev. 87, 387 (1952).

18. Herman, F.: J. Electronics 1, 103 (1955).

19. Amsterdam, M. F.: SCP and Solid State Tech., 15 (June 1964).

20. Cummerow, R. L.: Phys. Rev. 95, 16 (1954).

21. Oliver, J. W.: Space Tech. Lab., 8987-001-RU-001, 1962.

22. Lamorte, M. F.; and McIver, G. W.: Air Force contract No. AF 33(616)-6615, September 1962.

23. Development of Improved Gallium Arsenide Solar Cells, Final Report, Radio Corporation of America, NASA contract No. NAS 5-9006, February 1965.

24. Wysocki, J. J.: IEEE Transactions on Nuclear Science, 60 (November 1963).

VITA

Marvin Eddleman Beatty III

The author was born in Charlotte, North Carolina, July 5, 1940. He graduated from West Mecklenburg High School in that city, June 1958, Bachelor of Science in Nuclear Engineering, North Carolina State University, May 1962.

In September 1963, the author enrolled at the College of William and Mary as a graduate student in Physics.

TABLE I

PHYSICAL PROPERTIES OF GaAs AND Si

Properties	Si	GaAs
Melting point (°C)	1420	1238
Density (g/cm^3)	2.328	5.312
Liquid density (g/cm^3 at mp)		5.45
Lattice constant (A°)	5.431	5.634
Dist. between nearest neighbors (Å)	2.35	2.45
Atoms per cm^3 ($\times 10^{22}$)	4.99	4.43
Thermal coeff. of expansion (1°)	4.2×10^{-6}	5.93×10^{-6}
Pressure at mp (atm)	10^{-6}	0.9
Thermal conductivity (watt units)	0.84	0.52
Specific heat (cal/gm)	0.181	0.086
Latent heat of fusion (kcal/mole)	9.45	21 ± 3
Dielectric constant	11.7	11.1
Elastic moduli C_{11}	1.674	1.188
($\times 10^{12}$ dynes/cm^2) C_{12}	0.652	0.538
C_{44}	0.796	0.594
Volume compressibility ($\times 10^{-12}$ cm^2/degree)	0.98	
Magnetic susceptibility (cgs)	-0.13×10^{-6}	
Debye temperature (°K)	652	
Emissivity (1200° C)	~ 0.5	
Band gap (25° C)	1.106	1.40
Temp. dep. of band gap (eV/°C)	-4.4×10^{-4}	-4.5×10^{-4}
Electron lattice mobility (cm^2/V-sec)	1900	12000
Hole lattice mobility	425	450
Temp. dep. electron lattice mobility	T-2.5	~T-1
Temp dep. hole lattice mobility	T-2.7	T-2.1
Electron effective mass ratio	1.1	0.072
Hole effective mass ratio	0.59	0.5
Intrinsic electrons (25° C) (cm^{-3})	1.5×10^{10}	1.4×10^{6}
Intrinsic resistivity (25°) (ohm-cm)	2.3×10^{5}	3.7×10^{8}
Energy gap, eV (type)	indirect	direct
Refractive index, N	3.42	3.34
Work function, eV	5.05	4.66

TABLE II

UNIFORMITY OF POST BOMBARDMENT LIFETIMES

IN SILICON AND GALLIUM ARSENIDE

	Flux, 22-MeV protons/cm^2					
Sample	0	3×10^{10}	7×10^{10}	1×10^{11}	5×10^{11}	5×10^{12}
Type	Lifetime, microseconds					
P-type Si						
No. 1	4.4	2.04	1.13	0.57	0.24	0.03
No. 2	4.3	2.12	1.24	0.75	0.31	0.04
No. 3	3.3	2.00	0.93	0.50	0.23	0.03
No. 4	4.4	2.06	0.98	0.48	0.21	0.03
N-type Si						
No. 1	2.9	0.53	0.22	0.10	0.04	0.001
No. 2	3.3	0.55	0.25	0.11	0.04	0.001
No. 3	2.3	0.47	0.23	0.09	0.03	0.001
No. 4	4.1	1.20	0.64	0.28	0.10	0.01
	Flux, 40-MeV protons/cm^2					
P-type Si	0	5×10^{10}	1×10^{11}	5×10^{11}	1×10^{12}	5×10^{12}
No. 5	11.0	6.0	4.5	3.3	2.4	1.0
No. 6	10.0	-	4.4	2.8	1.7	1.0
No. 7	10.0	5.5	4.3	2.6	1.7	-
No. 8	11.0	5.8	4.5	3.6	2.5	-
N-type Si						
No. 5	6.0	3.0	2.0	0.61	0.40	0.13
No. 6	5.0	2.4	1.7	0.50	0.30	0.10
No. 7	4.0	1.9	1.3	0.48	0.28	0.09
No. 8	4.0	1.8	1.1	0.45	0.28	0.09

TABLE II (Continued)

	Flux, 22-MeV protons/cm^2				
	0	4.5×10^{12}	1×10^{13}	5×10^{13}	1×10^{14}
N-type GaAs No. 1	79.0	71.0	60.0	30.0	19.0
No. 2	55.0	42.0	36.0	25.0	18.0
No. 3	63.0	49.0	42.0	25.0	18.0
No. 4	65.0	51.0	43.0	22.0	15.0
	Flux, 40-MeV protons/cm^2				
N-type GaAs No. 1	67.0	48.0	36.0	24.0	18.0
No. 2	56.0	40.0	35.0	27.0	19.0
No. 3	50.0	42.0	36.0	29.0	18.0
No. 4	27.0	27.0	20.0	15.0	12.0